

國立臺灣大學獸醫專業學院臨床動物醫學研究所

碩士論文

Graduate Institute of Veterinary Clinical Science School of Veterinary  
Medicine

National Taiwan University

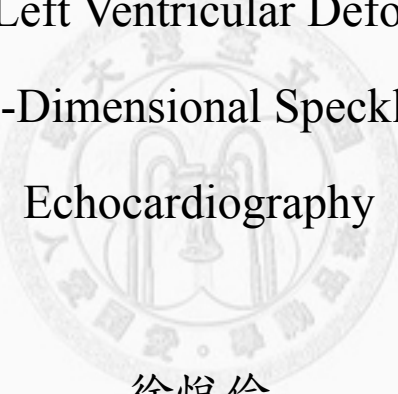
Master Thesis

以二維斑點追蹤心臟超音波評估貓之左心室運動

Assessment of Left Ventricular Deformation in Cats

Using Two-Dimensional Speckle Tracking

Echocardiography



徐悅倫

Yueh-Lun Hsu

指導教授：黃慧璧博士

Advisor : Hui-Pi Huang, DVM, Ph.D

中華民國 101 年 7 月

July, 2012

國立臺灣大學（碩）博士學位論文  
口試委員會審定書

以二維斑點追蹤心臟超音波評估貓之左心室運動

Assessment of Left Ventricular Deformation in  
Cats Using Two-Dimensional Speckle Tracking  
Echocardiography

本論文係徐悅倫君（R98643005）在國立臺灣大學獸醫學系、所完成之碩士學位論文，於民國 101 年 07 月 18 日承下列考試委員審查通過及口試及格，特此證明

口試委員：

黃慧璧

（簽名）

（指導教授）

吳文亭

林菊龍

系主任、所長

吳文亭

（簽名）

## Acknowledgment

謝謝爸爸，能夠在這個階段獨立成人，沒有顧忌的往前努力，就是因為爸爸無怨無悔幾十年的付出，這份恩惠實在不能僅用文字表達。

謝謝我的老師，黃慧璧老師，在動物醫學的研究、臨床領域中表現的謙虛、並且堅持的態度是我的典範，不厭其煩的教導與討論，啟蒙了我很多。

謝謝小五，你是我投入這個領域，並且繼續在這個領域中繼續努力的主要原因，更是我選擇獸醫系後獲得的最大禮物，彷彿唸這個系，就是為了與你相遇。

謝謝我的同窗，虹吟、子綺、秉燁、阿花、彥貞，這三年來的點點滴滴，很辛苦但卻沒有成為痛苦的時光，就是因為有你們可以一起抱怨，一起難過和一起開心。

謝謝我的朋友，對我不求回報的付出，每每讓我覺得一生中怎麼有幸可以認識這麼多真摯的人。特別謝謝葉狗狗，在大雨中騎摩托車載著兩隻貓讓我掃超音波，義不容辭的幫忙讓我非常感動和感激。

謝謝八年來遇到的動物們，你們用生命帶給人類幸福，希望在醫學上可以好好的報答，並且能讓更多人可以繼續愛護你們。

謝謝。

## Abstract

Two-dimensional speckle tracking echocardiography (2D-STE) applies the special corrugated of constructive interference and destructive interference when ultrasound passes through myocardial tissue to locate myocytes. This modality is able to calculate myocardial deformation, strain and strain rate (SR), synchrony and heterogeneity.

This thesis contains two studies. The first study established 2D-STE of strain, SR, synchrony and heterogeneity of clinically normal cats, physiological characteristics might affect the indices derived from 2D-STE were analyzed, and the correlation between 2D-STE and conventional echocardiography were also evaluated. In the second study left ventricular function of clinically normal cats and cats with lower respiratory tract diseases was assessed using 2D-STE.

In general, strain, SR, synchrony and heterogeneity derived by 2D-STE were almost not influenced by age, body weight, heart rate and blood pressure, but affected by gender. In clinically healthy cats, segmental and transmural heterogeneity were evidenced in myocardial deformation. The correlation between 2D-STE indices and conventional echocardiography were weak. It is implied that 2D-STE was more sensitive in detection of left ventricular dysfunction. In terms of decreased myocardial strain and SR, mild systolic and diastolic dysfunction was found in cats with lower respiratory tract diseases, and it might be caused by the mechanism other than ventricular interdependence.

## 摘要

二維斑點追蹤心臟超音波利用超音波在心肌細胞內產生的建設性干涉和破壞性干涉的特殊波紋，對心肌進行定位，進一步計算位移和形變量、形變率，比起傳統超音波利用整體容積形變或壓力差為基礎，測量估計心臟整體收縮力，斑點追蹤心臟超音波可以達到局部心臟收縮力的評估。局部心臟收縮力的表現包括形變量和形變率，綜合各個局部心臟收縮力的表現可進一步評估收縮的同步性和異質性。

本篇論文有兩個章節，第一章節以建立二維斑點追蹤超音波應用於臨床上健康貓計算左心運動形變量、形變率、同步性和異質性的範圍為目的，了解生理因子是對於這些數值的影響，以及二維斑點追蹤超音波計算出的局部收縮力和傳統超音波計算出的整體收縮功能的關聯。第二章節應用二維斑點追蹤心臟超音波比較下呼吸道疾病貓和臨床健康貓隻的左心功能改變。

總體來說，二維斑點追蹤心臟超音波計算出的形變指數，同步性和異質性不受到年齡、體重、心跳、血壓影響，但存在性別差異；並且證實臨床健康貓的心肌運動具有跨壁和節段形變量的異質性；二維斑點超音波的形變指數和傳統超音波的功能指數關連性低，顯示心肌局部功能的改變可能受到其他區域的心肌運動代償，因而傳統超音波的整體功能測量敏感性較低。下呼吸道疾病貓隻的左心形變量偏低，顯示左心收縮、舒張功能受到影響，應該是藉由心室間關聯性以外的機制造成。

## Table of Contents

	口試委員審定書	i
	Acknowledgment	ii
	Abstract	iii
	摘要	iv
	Table of Contents	v
	List of Tables	vi
	List of Figures	viii
Chapter I	General Introduction	1
	References	8
Chapter II	Two-Dimensional Speckle Tracking Echocardiographic Assessment of Mechanical Ventricular Synchrony and Heterogeneity in Clinically Normal Cats	13
	References	28
Chapter III	Comparison between Conventional and Two Dimensional Speckle-Tracking Echocardiography in Clinically Healthy Cats and Cats Affected with Lower Respiratory Tract Disease	46
	References	58
Chapter IV	Summarized Discussion	69
	References	71

## List of Tables

### Chapter II

Table 1.	The descriptive statistics of the population characteristic and conventional echocardiography indices of 34 clinically healthy cats	33
Table 2.	The intra-observer coefficient of variance (CV) of 2D-STE variables	35
Table 3.	Circumferential, radial and longitudinal strain and systolic strain rate values for regional left ventricular segments determined using two-dimensional speckle tracking echocardiography in 34 clinical healthy cats	36
Table 4.	Characteristics of cats and indices of strain and strain rate	37
Table 5.	Relationship between indices derived from conventional echocardiography and strain and strain rate	38
Table 6.	Relationship between indices derived from Doppler echocardiography and strain and strain rate	40
Table 7.	Descriptive statistics of ventricular heterogeneity and synchrony in clinically healthy cats	41
Table 8.	Characteristics of cats and ventricular synchrony (RT- $\epsilon$ , SDT- $\epsilon$ ) and heterogeneity (SH- $\epsilon$ , TH-c $\epsilon$ )	41
Table 9.	Relationship between indices derived from conventional echocardiography and left ventricular synchrony and heterogeneity	42
Table 10.	Comparison MEVp, MAVp, M <sub>E/A</sub> , TEVp, TAVp, T <sub>E/A</sub> , Q <sub>P-A0</sub> , IVRT, Tei index with heterogeneity (SH- $\epsilon$ , TH- $\epsilon$ ) synchrony (RT- $\epsilon$ , SDT- $\epsilon$ )	44
Table 11.	Relationship between indices of strain and strain rate and left ventricular synchrony and heterogeneity	45

### Chapter III

Table 1.	Comparison of demographics between clinically healthy cats (control) and acts with lower respiratory tract disease (LRTD)	62
Table 2.	Comparison of left ventricular indices between clinically healthy cats (control) and acts with lower respiratory tract	63

	disease (LRTD)	
Table 3.	Comparison of indices derived from conventional echocardiography between clinically healthy cats (control) and acts with lower respiratory tract disease (LRTD)	64
Table 4.	Comparison of circumferential strain and strain rate between clinically healthy cats (control) and acts with lower respiratory tract disease (LRTD)	65
Table 5.	Comparison of radial strain and strain rate between clinically healthy cats (control) and acts with lower respiratory tract disease (LRTD)	66
Table 6.	Comparison of longitudinal strain and strain rate between clinically healthy cats (control) and acts with lower respiratory tract disease (LRTD)	67
Table 7.	Comparison of left ventricular ejection volume ( $EF_{ste}$ ) and fraction area change (FAC) between clinically healthy cats (control) and cats with lower respiratory tract disease (LRTD)	68
Table 8.	Comparison of ventricular synchrony (RT-c $\epsilon$ , SDT-c $\epsilon$ ) and heterogeneity (SH- $\epsilon$ and TH- $\epsilon$ ) between clinically healthy cats (control) and cats with lower respiratory tract disease (LRTD)	68

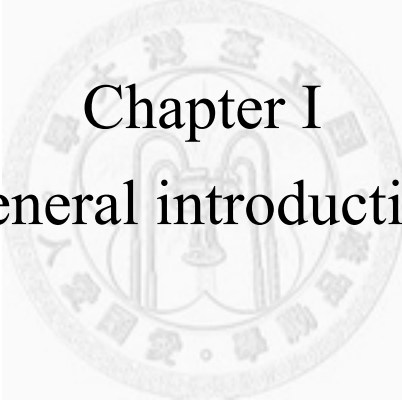


## List of Figures

### Chapter I.

- |           |   |    |
|-----------|---|----|
| Figure 1. | Mathematical relationship between different deformation parameters and mode of calculation for speckle tracking echocardiography (STE) and tissue Doppler imaging (TDI), STE primary assess myocardial displacement, whereas TDI primarily assesses tissue velocity | 10 |
| Figure 2. | Definition of strain and shear strain   | 11 |
| Figure 3. | Local heart coordinate system: Sampling a cubic myocardium, and analysis the deformation in Cartesian coordinate system with circumferential, radial and longitudinal orientation   | 12 |
| Figure 4. | Illustration of regional myocardium forced status   | 12 |





# Chapter I

## General introduction

### Key to abbreviations

LV	Left ventricular
STE	Speckle tracking echocardiography
TDI	Tissue Doppler imaging
$\varepsilon$	Lagrangian strain
$\varepsilon_N$	Eulerian strain



## **Introduction**

Echocardiographic imaging is ideally suited for the evaluation of cardiac mechanics because of its intrinsically dynamic nature. Speckle tracking echocardiography (STE) is a technology development in the decade. In contrast to tissue Doppler imaging, there is no dependency of the measurements on the insonation angle between the ultrasound beam and the direction of motion. Speckle tracking echocardiography is also a non-invasive and less cost examination compared to tagged magnetic resonance imaging or sonomicrometry.

## **Continuum mechanics— Context of cardiac mechanics**

### *Langrangian description & Eulerian description —Speckle tracking echocardiography & tissue Doppler imaging*

The continuum mechanical description of material relies on the characterization of material motion through space and time. The variation in observed motion within a material depends strongly on a reference frame. There are two methods for describing deformation on a continuum [1-3].

One description is made in terms of the material description. This is called “material description” or “Lagrangian description”, which defines motion around a given point in tissue as it traverses through space and time. Speckle-tracking echocardiography analyzes Lagrangian strain, in which the end-diastolic tissue dimension represents the unstressed, initial material length as a fixed reference throughout the cardiac cycle [1-3].

Another description is made in terms of the spatial coordinates. This is also called the “spatial description” or “Eulerian description”. It describes deformation by considering the relative velocity of motion at a particular location in space as despite

time goes by. Tissue Doppler imaging (TDI) analyzes Eulerian strain (Fig. 1) [1-3].

## Definitions of strain and strain rate

### Strain –Langarian strain & Eulerian strain

Langarian strain ( $\epsilon$ ) is mathematically defined as the change of myocardial fiber length during stress at end-systole  $L(t)$  compare to its original length in a relaxed state at end-diastole,  $L(t_0)$ . In one-dimensional object, the only possible deformation of the object is lengthening or shortening.

$$\epsilon(t) = \frac{L(t) - L(t_0)}{L(t_0)}$$

Strain is usually expressed in percent (%).

Eulerian strain ( $\epsilon_N$ ) is described expressed relative to the length at a previous time instance:

$$d\epsilon_N(t) = \frac{L(t+dt) - L(t)}{L(t)}$$

$$\epsilon_N(t) = \int_{t_0}^t d\epsilon_N(t)$$

The reference value is not constant over time bit changes during the deformation process. The Lagrangian strain  $\epsilon$  and the Eulerian strain  $\epsilon_N$  have a fixed, but non-linear, relationship which is given by  $\epsilon_N(t) = \ln(1 + \epsilon(t))$ .

If strains are small (of the order 5-10%) Lagrangian and Eulerian strain values are approximately equal. However, for the large deformations which can occur during cardiac ejection and rapid filling, the differences become significant [1, 3-5].

### Strain –Normal strain & shear strain

As with stresses, strains may also be classified as 'normal strain' and 'shear strain'. In other words, normal strain is the deformation acting along the direction of stress and shear strain is the deformation acting perpendicular to the direction of stress (Fig.

2) [3, 4, 6].

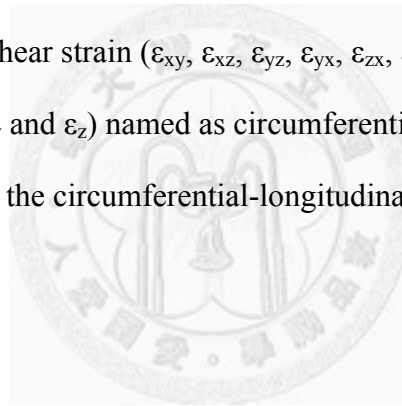
### Strain rate

The change of strain per unit of time is referred to as strain rate. As strain rate is the spatial derivative of tissue velocity (mm/s) in, and strain (%) is the temporal integral of strain rate, all of these three parameters are mathematically linked to each other by method of STE and TDI (Fig. 1) [3, 4, 7].

### **Regional myocardial coordinate system**

To decompose the cubic regional myocardial deformation of 3 directions by using Cartesian coordinates (Fig.3), including three direction of normal strain ( $\epsilon_x$ ,  $\epsilon_y$  and  $\epsilon_z$ ) and 6 direction of shear strain ( $\epsilon_{xy}$ ,  $\epsilon_{xz}$ ,  $\epsilon_{yz}$ ,  $\epsilon_{yx}$ ,  $\epsilon_{zx}$ ,  $\epsilon_{zy}$ ).

The 3 normal strains ( $\epsilon_x$ ,  $\epsilon_y$  and  $\epsilon_z$ ) named as circumferential, radial and longitudinal strain. Myocardial shear in the circumferential-longitudinal plane results in twist or torsion [2, 3].



### **Structural mechanics**

“We cannot claim to have mastered the mechanism of the human heart until we have a fundamental explanation of its architecture.”— stated by Keith in 1918.

Studies have pointed out that heart is a band of muscle, which consist of 4 segments, circumferential fiber right/left segments, descending segments(right-handed helix), ascending(left-handed helix)-Torrent-Guasp’s model [8]. The band of muscle twines like a figure-of-eight-knot. Therefore, LV free wall is compatible with overlapping myocardial segments that are discontinuous or separated by a narrow zone in which fiber angles change markedly over very short distance.

In contrast to Streeter model of heart, cardiac wall is a continuum of fiber angles

across the wall, the fiber located at subendocardial region shows right-handed helical myofiber geometry, which changes gradually into a left-handed helical geometry in the subepicardium. Thus, the subendocardium, the fibers are roughly longitudinally oriented with an angle of about  $80^\circ$  with respect to the circumferential direction. The angle decreases toward the midwall, where the fibers are oriented in the circumferential direction ( $0^\circ$ ), and decreases further to an oblique of about  $-60^\circ$  in the subepicardium [7-9].

The common feature of a circumferential muscle mass with predominantly transverse fibers and the oblique helical fiber arrangement of the inner and outer wall are documented by all anatomic descriptions and must be integrated by all functional models that can explain how the heart fills and empties [8].

### **Regional cardiac mechanics**

The regional myocardial mechanics can simply by application the theory of physical tension to simulate myocardial forced status.

Regional myocardial stress state can be explained as the following formula [10, 11]:

Wall stress<sub>passive</sub> (t) – contractile force<sub>active</sub> (t) = elasticity x deformation (t)

There is a Heart filled with blood (Fig. 4) and we analyzed a small area A at the cardiac surface of force status. Therefore, the main factors influencing regional myocardial deformation are:

1. Cardiac wall stress from intracardiac blood pressure (loading)
2. Intrinsic contractile force developed by myocardium
3. Interaction between area A with other neighboring area (tension)
4. Tissue properties (elasticity)

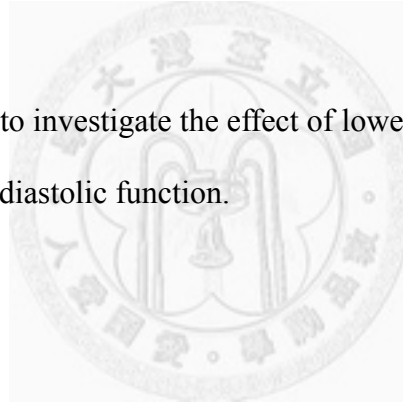
For example, the more loading of heart rely on the greater tension from

neighboring area interaction. Thence, myocardial deformation evaluated by STE cannot fully express the myocardial contractility, but it is the closest method to the assessment of contractile forces among current multiple fashion.

### **Aims**

The aims of this study were application of speckle tracking echocardiography to assess left ventricular deformation in feline, establish of repeatability and reproducibility in speckle tracking echocardiography, outline the baseline range of normal strain(circumferential, radial and longitudinal) and heterogeneity/ synchrony, determine physiologic factor effects and understand the correlation with conventional echocardiography.

Further apply of STE to investigate the effect of lower respiratory tract disease on left ventricular systolic/diastolic function.





## References

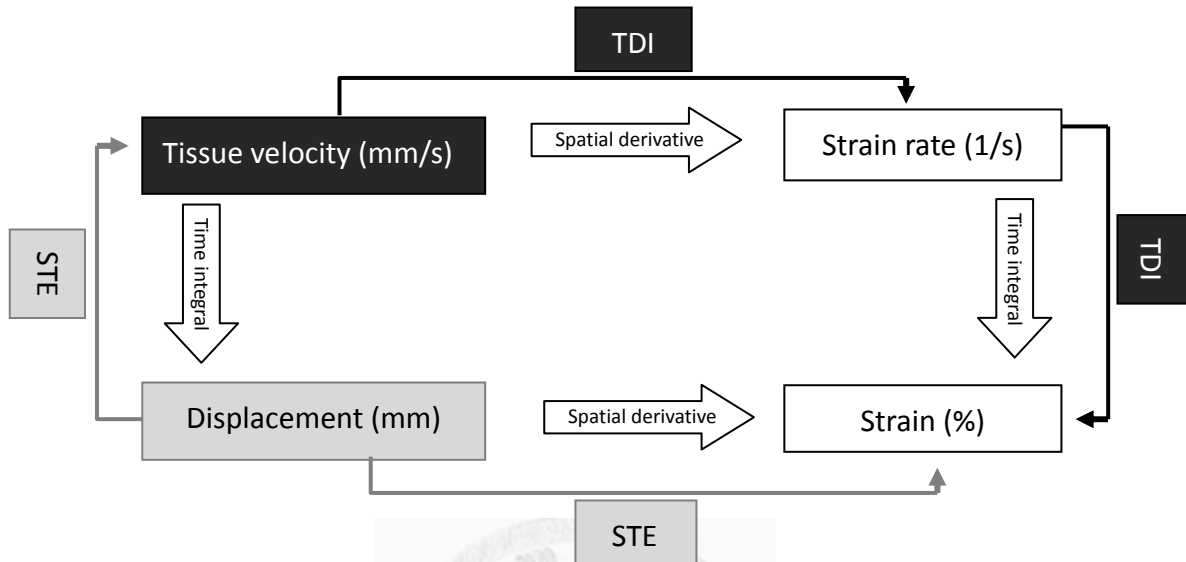
1. Nordsletten DA, Niederer SA, Nash MP, Hunter PJ, Smith NP: **Coupling multi-physics models to cardiac mechanics**. *Prog Biophys Mol Biol* 2011, **104**:77-88.
2. Geyer H, Caracciolo G, Abe H, Wilansky S, Carerj S, Gentile F, Nesser HJ, Khandheria B, Narula J, Sengupta PP: **Assessment of myocardial mechanics using speckle tracking echocardiography: fundamentals and clinical applications**. *J Am Soc Echocardiogr* 2010, **23**:351-369; quiz 453-355.
3. D'hooge J, Heimdal A, Jamal F, Kukulski T, Bijnens B, Rademakers F, Hatle L, Suetens P, Sutherland G: **Regional strain and strain rate measurements by cardiac ultrasound: principles, implementation and limitations**. *Eur J Echocardiogr* 2000, **1**:154-170.
4. Blessberger H, Binder T: **NON-invasive imaging: Two dimensional speckle tracking echocardiography: basic principles**. *Heart* 2010, **96**:716-722.
5. Pavlopoulos H, Nihoyannopoulos P: **Strain and strain rate deformation parameters: from tissue Doppler to 2D speckle tracking**. *Int J Cardiovasc Imaging* 2008, **24**:479-491.
6. Teske AJ, De Boeck BW, Melman PG, Sieswerda GT, Doevendans PA, Cramer MJ: **Echocardiographic quantification of myocardial function using tissue deformation imaging, a guide to image acquisition and analysis using tissue Doppler and speckle tracking**. *Cardiovasc Ultrasound* 2007, **5**:27.
7. Mor-Avi V, Lang RM, Badano LP, Belohlavek M, Cardim NM, Derumeaux G, Galderisi M, Marwick T, Nagueh SF, Sengupta PP, Sicari R, Smiseth OA, Smulevitz B, Takeuchi M, Thomas JD, Vannan M, Voigt JU, Zamorano JL: **Current and evolving echocardiographic techniques for the quantitative evaluation of cardiac mechanics: ASE/EAE consensus statement on methodology and indications endorsed by the Japanese Society of Echocardiography**. *Eur J Echocardiogr* 2011, **12**:167-205.
8. Buckberg G, Hoffman JI, Mahajan A, Saleh S, Coghlan C: **Cardiac mechanics revisited: the relationship of cardiac architecture to ventricular function**. *Circulation* 2008, **118**:2571-2587.
9. Streeter DDJ: **Gross morphology and fiber geometry of the heart**. In **Handbook of Physiology**. In *Handbook of Physiology. Volume 1*. 1st edition. Edited by Berne RM, Sperelakis N, Geigert SR. Washinton, DC: American Physiological Society; 1979:61-112.
10. Bijnens B, Cikes M, Butakoff C, Sitges M, Crispi F: **Myocardial motion and deformation: what does it tell us and how does it relate to function**. *Fetal*

*Diagn Ther* 2012, **32**:5-16.

11. Bijmens BH, Cikes M, Claus P, Sutherland GR: **Velocity and deformation imaging for the assessment of myocardial dysfunction.** *Eur J Echocardiogr* 2009, **10**:216-226.



**Fig. 1** Mathematical relationship between different deformation parameters and mode of calculation for speckle tracking echocardiography (STE) and tissue Doppler imaging (TDI), STE primary asses myocardial displacement, whereas TDI primarily assesses tissue velocity.

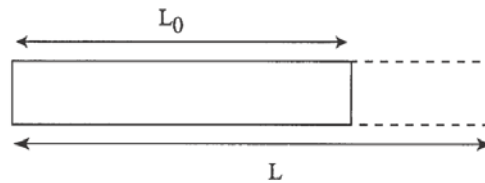


Adapted from "NON-invasive imaging: Two dimensional speckle tracking echocardiography: basic principles" by H. Blessberger and T. Binder, 2010, *Heart*, 96, p.716-722. Copyright 2000 by BMJ Publishing Group Ltd & British Cardiovascular Society.

**Fig. 2** Definition of strain and shear strain.

**Strain at one-dimension**

Change of myocardial fiber length during stress at end-systole (L) compare to its original length in a relaxed state at end-diastole (L<sub>0</sub>).

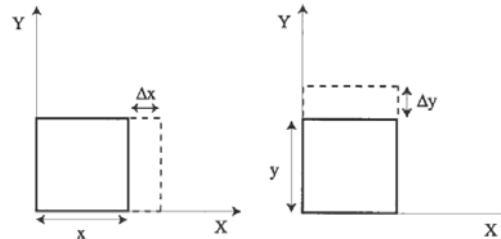


**Normal strain at two-dimension**

Deformation along the stress

$$\epsilon_x = \frac{\Delta x}{x} \quad (\text{left, stress direction, } x)$$

$$\epsilon_y = \frac{\Delta y}{y} \quad (\text{right, stress direction, } y)$$

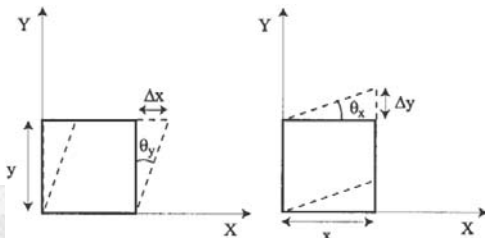


**Shear strain at two-dimension**

Deformation perpendicular the stress

$$\epsilon_{xy} = \frac{\Delta x}{y} \quad (\text{left, stress direction, } y)$$

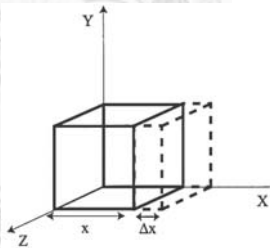
$$\epsilon_{yx} = \frac{\Delta y}{x} \quad (\text{right, stress direction, } x)$$



**Normal strain at three-dimension**

Deformation along the stress

$$\epsilon_x = \frac{\Delta x}{x} \quad (\text{stress on the } yz \text{ plane})$$

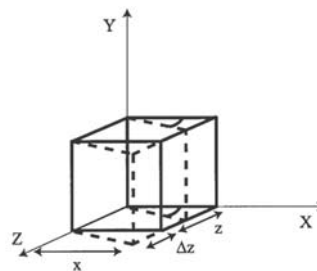
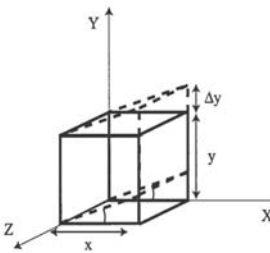


**Shear strain at three-dimension**

Deformation perpendicular the stress

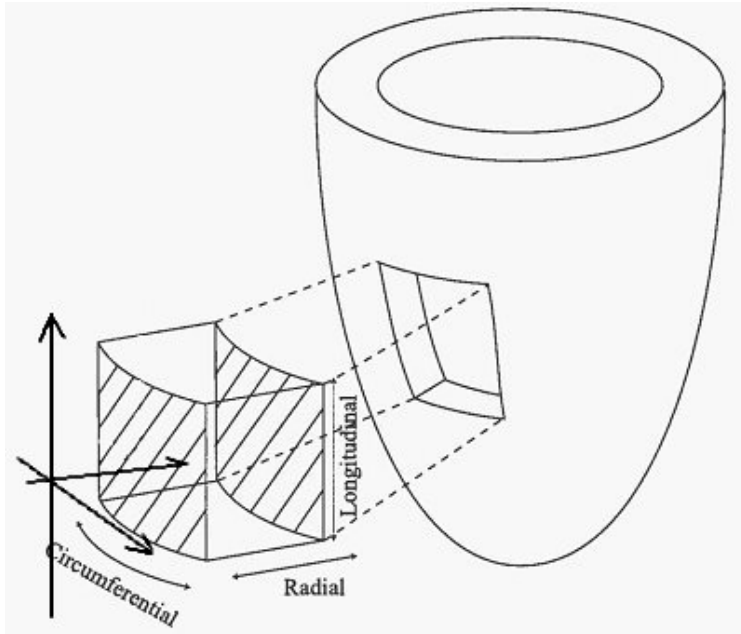
$$\epsilon_{yx} = \frac{\Delta y}{x} \quad (\text{upper, stress on the } yz \text{ plane})$$

$$\epsilon_{zx} = \frac{\Delta z}{x} \quad (\text{lower, stress on the } yz \text{ plane})$$



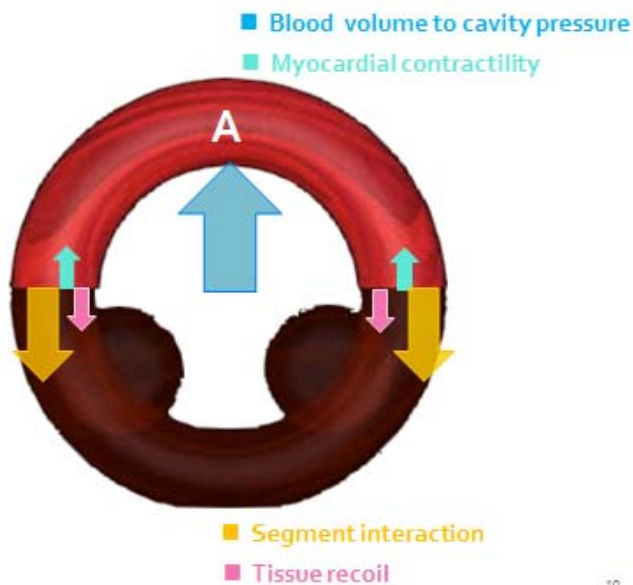
Adapted from "Regional strain and strain rate measurements by cardiac ultrasound: principles, implementation and limitations" by J. D'hooge and A. Heimdal, 2000, *Eur J Echocardiogr*, 1, p. 154-170. Copyright 2000 by the European Society of Cardiology.

**Fig. 3** Local heart coordinate system: Sampling a cubic myocardium, and analysis the deformation in Cartesian coordinate system with circumferential, radial and longitudinal orientation.



Adapted from "Regional strain and strain rate measurements by cardiac ultrasound: principles, implementation and limitations" by J. D'hooge and A. Heimdal, 2000, *Eur J Echocardiogr*, 1, p.154-170. Copyright 2000 by the European Society of Cardiology.

**Fig. 4** Illustration of regional myocardium forced status.

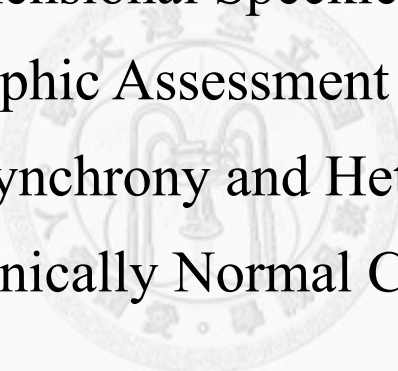


Segment A of myocardium maintain the balance of tension with blood pressure, intrinsic contractility, tissue recoil stress and segmental interaction. Adapted from "Velocity and deformation imaging for the assessment of myocardial dysfunction" by B.H. Bijnens and M. Cikes, 2009, *Eur J Echocardiogr*, 10, p.216-226. Copyright 2008 by the European Society of Cardiology.

20

Chapter II

Two-Dimensional Speckle Tracking  
Echocardiographic Assessment of Mechanical  
Ventricular Synchrony and Heterogeneity in  
Clinically Normal Cats



### Key to abbreviations

2D-STE	Two-dimensional speckle tracking echocardiography
AAT	Aortic outflow acceleration time
AGp	Aortic outflow peak velocity pressure gradient
AVp	Aortic outflow peak velocity
BW	Body weight
CS	Peak circumferential strain
CSg	Global peak circumferential strain
CSR	Peak circumferential systolic strain rate
CSR <sub>-A</sub>	Peak circumferential late diastolic strain rate
CSR <sub>-Ag</sub>	Global peak circumferential late diastolic strain rate
CSR <sub>-E</sub>	Peak circumferential early diastolic strain rate
CSR <sub>-Eg</sub>	Global peak circumferential early diastolic strain rate
CSRg	Global peak circumferential systolic strain rate
EF <sub>M</sub>	Ejection fraction derived from m-mode
EF <sub>ste</sub>	Ejection fraction derived from speckle tracking echocardiography
EPSS	E point to septal separation
ESVI	End systolic volume index
FAC	Fractional area change
FS	Fractional shortening
HR	Heart rate
IVRT	Isovolumic relaxation time
IVS%	Percentage thickening of the interventricular septum
IVSd	Interventricular septal thickness in end diastole
LA/Ao	The ratio of left atrium and aortic diameter
LS	Peak longitudinal strain
LSg	Global peak longitudinal strain
LSR	Peak longitudinal systolic strain rate
LSR <sub>-A</sub>	Peak longitudinal late diastolic strain rate
LSR <sub>-Ag</sub>	Global peak longitudinal late diastolic strain rate
LSR <sub>-E</sub>	Peak longitudinal early diastolic strain rate
LSR <sub>-Eg</sub>	Global peak longitudinal early diastolic strain rate
LSRg	Global peak longitudinal systolic strain rate
LVDd	Left ventricular dimension in end-diastole
LVDs	Left ventricular dimension in end-systole
LVPW%	Percentage thickening of the left ventricular free wall
LVPWd	Left ventricular free wall thickness in end-diastole

LVFWs	Left ventricular free wall thickness in end-systole
LVMI	Left ventricular mass index
MAvp	Peak late mitral inflow velocity
M <sub>E/A</sub>	Early and late mitral inflow ratio
MEVp	Peak early mitral inflow velocity
PEP:ET	Pre-ejection time period and ejection time ratio
PVp	Pulmonary outflow peak velocity
Q <sub>P-Ao</sub>	Difference between pulmonary pre-ejection time and aortic pre-ejection time
RS	Peak radial strain
RSg	Global peak radial strain
RSR	Peak radial systolic strain rate
RSR <sub>-A</sub>	Peak radial late diastolic strain rate
RSR <sub>-Ag</sub>	Global peak radial late diastolic strain rate
RSR <sub>-E</sub>	Peak radial early diastolic strain rate
RSR <sub>-Eg</sub>	Global peak radial early diastolic strain rate
RSRg	Global peak radial systolic strain rate
RT-cε	Range of the 6 segment time to peak circumferential strain
RT-lε	Range of the 6 segment time to peak longitudinal strain
RT-rε	Range of the 6 segment time to peak radial strain
RT-ε	Range of the 6 segment time to peak strain
SDT-cε	Standard deviation of the 6 segment time to peak circumferential strain
SDT-lε	Standard deviation of the 6 segment time to peak longitudinal strain
SDT-rε	Standard deviation of the 6 segment time to peak radial strain
SDT-ε	Standard deviation of the 6 segment time to peak strain
Sg	Global peak strain
SH-cε	Circumferential segmental heterogeneity
SH-lε	Longitudinal segmental heterogeneity
SH-rε	Radial segmental heterogeneity
SH-ε	Segmental heterogeneity
SR	Peak systolic strain rate
SR <sub>-A</sub>	Peak late diastolic strain rate
SR <sub>-Ag</sub>	Global peak late diastolic strain rate
SR <sub>-E</sub>	Peak early diastolic strain rate
SR <sub>-Eg</sub>	Global peak early diastolic strain rate
SRg	Global peak strain rate
SV	Stroke volume



TAVp	Peak late tricuspid inflow velocity
T <sub>E/A</sub>	Early and late tricuspid inflow ratio
Tei index	Myocardial performance index
TEVp	Peak early tricuspid inflow velocity
TH-ε	Transmural heterogeneity
Vcf	Velocity of circumferential fiber shortening
ε	Langarian strain



## **Two-Dimensional Speckle Tracking Echocardiographic Assessment of Mechanical Ventricular Synchrony and Heterogeneity in Clinically Normal Cats**

Yueh-Lun Hsu, Hui-Pi Huang

Department of Veterinary Medicine, National Taiwan University, Taipei, Taiwan

### **Abstract**

Two-dimensional speckle tracking echocardiography (2D-STE) makes the regional cardiac deformation and function can be evaluated. Regional myocardial synchrony and heterogeneity in the human cardiac disease can be featured as pathogenesis or the consequence of specific diseases.

The aims of this study were firstly to assess the reproducibility and reproducibility of 2D-STE in clinical healthy feline, secondly to determine the influence of physical characteristic (age, body weight, heart rate, sex and blood pressure) in strain, strain rate (SR), synchrony/heterogeneity of left ventricle, and thirdly to compare the indices derived from 2D-STE with hemodynamic analysis obtained by conventional echocardiography.

Thirty-three clinical healthy cats were included. Both standard conventional echocardiography and 2D-STE were performed. Indices of circumferential, radial and longitudinal strain and SR, synchrony and heterogeneity were collected.

Indices of 2D-STE were almost free from the influence of physiological factors, but there were presence of gender differences. The deformations of left ventricle in clinically healthy cats possess heterogeneity, which the longitudinal strain/SR was lower in apex and circumferential strain was decreasing from subendocardium to subepicardium. Indices derived from 2D-STE were not correlated to M-mode indices of conventional echocardiography, and weakly correlated to pulse-wave Doppler indices. It is implied that regional deformation alteration may compensate by each other and makes 2D-STE more sensitive in detection of left ventricular dysfunction. Meanwhile, systolic strain or SR was correlated to diastolic indices in conventional echocardiography. It is indicated that the boundary of diastolic and systolic function in the regional deformation may not be aware. Need more diseases and health research or longitudinal study in order to further understand the significance of the deformation.

Key words: two-dimensional speckle tracking echocardiography, heterogeneity, synchrony, feline

---

Part of the study is going to present as an abstract in the 22<sup>nd</sup> European College of Veterinary Internal Medicine Congress, Maastricht, the Netherlands. Sep. 6-8, 2012.

## **Introduction**

Ventricular contraction normally occurs in a highly coordinated process. Diseased myocardium is usually resulted from impaired electrophysiological activity (electrical dyssynchrony), and induce electrical conduction delay [1, 2]. Non-uniform in timing of electromechanical activation in different areas of the myocardium can produce myocardial contraction dyssynchrony (mechanical dyssynchrony) [3, 4].

In recent years, ventricular dyssynchrony are found to be associated with causes and consequence both valvular insufficiency and myocardial disease in human patients [5-7]. Cardiac failure would amplify the regional stress disparities that result from discoordinate activation, and this may be an important interaction [8].

Dyssynchrony may induce asymmetric ventricular hypertrophy and alterations in regional myocardial blood flow [8, 9]. Mitral regurgitation, caused by delay in both the rise in left ventricular pressure and discoordinate papillary muscle contraction, can exacerbate this inefficiency further [8]. Presence of dyssynchronous ventricular contraction is an independent predictor of worsening heart failure [10, 11].

Quantification of ventricular synchrony and heterogeneity in clinical healthy cats is an essential first step in assessment of ventricular synchrony in cats. The aims of this study are to investigate left ventricular synchrony and heterogeneity in clinically healthy cats using two dimensional speckle tracking echocardiography (2D-STE).

## **Material and Method**

### ***Animals***

Thirty three client-owned cats admitted to the National Taiwan University Veterinary Hospital during 2010-2012 were included for this perspective study. Without history of respiratory or cardiac disease, all cats were deemed to be clinically

healthy based on physical examination, blood pressure measurements, routine blood work (complete blood counts and biochemical profiles), chest radiographs and conventional echocardiography. The mean age was  $3.11 \pm 2.17$  years (range 6 months to 8 years old) and a mean body weight was  $4.32 \pm 1.32$  kg, 18 were males, and 16 were females. The represented breeds were 19 Domestic Short-hairs, 6 American Short-hairs, 7 Persians, 1 Bengal cat and 1 British Blue.

### ***Measurement reliability***

All echocardiographic studies were performed by 1 examiner (YLH), using an ultrasound unit equipped with a 5.5-7.5 MHz phased-array transducer (MyLab<sup>TM</sup>50 XVision, Esaote, Genova, Italy).

STE examinations, including circumferential, radial and longitudinal orientation, of five clinical cats were acquired by one echocardiographer (YLH) thrice in one day to calculate intra-observer coefficient of variation. The resultant echocardiograms were analyzed by another investigator (BIY). Each variable was measured 3 times on 3 consecutive cardiac cycles using the same recorded loop. The intra-observer coefficient of variation (CV) was expressed as a percent value, calculated as  $CV = \text{Standard deviation} / \text{mean} \times 100\%$  in order to assess the repeatability of the measurements used in this study.

### ***Blood pressure***

Systemic blood pressure was measured by Doppler flow detector and an inflatable cuff attached to a sphygmomanometer which position between the carpal and metacarpal pad. Record the average result of 5 consecutive measurements.

### ***Conventional echocardiography***

Ultrasound examinations were performed without sedation in gently restrained cats in lateral recumbency [12].

Indices of left ventricle was including left ventricular diastolic dimension (LVDd), left ventricular systolic dimension (LVDs), the ratio of Left atrium and aortic diameter (LA/Ao), interventricular septal thickness in diastole (IVSd), left ventricular free wall thickness in diastole (LVFWd), and left ventricular mass index (LVMI) were obtained from the standard views [13, 14].

Parameters of left ventricular systolic function were derived from M-mode, including end-posterior E point to septal separation (EPSS), percentage thickening of the interventricular septum (IVS%), percentage thickening of the left ventricular free wall (LVFW%), fractional shortening (FS), ejection fraction by M-mode ( $EF_M$ ); parameters were derived from pulse-wave Doppler including velocity of circumferential fiber shortening (Vcf), the ratio of pre-ejection period an ejection time (PEP:ET), Aortic outflow acceleration time (AAT), including aortic outflow peak velocity (AVp), aortic outflow peak velocity pressure gradient (AGp), pulmonary outflow peak velocity (PVp), stroke volume (SV), and derived from B mode, including end systolic volume index (ESVI) were obtained from the standard views [14-23].

Parameters of left ventricular diastolic function were including mitral early and late diastolic inflow velocity (MEVp, MAVp), and tricuspid early and late diastolic inflow velocity (TEVp, TAVp), the ratio between MEVp and MAVp ( $M_{E/A}$ ), the ratio between TEVp and TAVp ( $T_{E/A}$ ), isovolumic relaxation time (IVRT), and myocardial performance index (Tei index) were obtained from the standard views [16, 24, 25].

Interventricular synchrony, the difference between pulmonary pre-ejection time and aortic pre-ejection time ( $Q_{P-Ao}$ ) was obtained from standard views [26].

### ***Two-dimensional speckle tracking echocardiography***

#### ***Measurement regional strain and strain rate***

Indices of left ventricular longitudinal and circumferential/radial/longitudinal strain and strain rates were obtained using right parasternal apical 4-chamber and short axis views, respectively. All images were acquired in cine loops of 3 cardiac cycles recorded at frame rate of 54-111 frames per seconds, saved in digital format, and analyzed by off-line software (XStrain<sup>TM</sup> software for MyLab<sup>TM</sup>50 X Vision).

In quantification of circumferential and radial strain and strain, 6 segments (cranio-septum, cranial, lateral, caudal, ventral, and septal) of endocardium were semi-automatically selected by Aided Heart Segmentation (AHS) for analysis. In left ventricular longitudinal strain and strain rate, 6 segments (basal-septal, mid-septal, apical-septal, apical-lateral, mid-lateral, basal-lateral) of endocardium were semi-automatically automatically selected by the AHS tool for analysis. Left ventricular ejection volume ( $EF_{ste}$ ) and fraction area change (FAC) were also calculated by modified Simpson's rule.

The 2D-STE indices included in this study were circumferential/radial/longitudinal peak systolic strain (CS/RS/LS), circumferential/radial/longitudinal peak systolic strain rate (CRS/RSR/LSR), circumferential/radial/longitudinal peak early diastolic strain rate ( $CSR_E/RSR_E/LSR_E$ ) and circumferential/radial/longitudinal peak late diastolic strain rate ( $CSR_A/RSR_A/LSR_A$ ). The 2D-STE off-line analysis was performed by 1 examiner (YLH).

The images without adequate visualization of one or more segments of the endocardium were excluded from this study.

#### ***Measurement of synchrony and heterogeneity***

Interventricular synchrony, defined as time difference between mean pulmonary and aortic pre-ejection periods ( $Q_{P-A_0}$ ), was calculated based on conventional pulse

wave-Doppler.

Intraventricular synchrony, defined as the standard deviation of the six segments time to reach peak strain (SDT- $\epsilon$ ) at longitudinal (SDT-l $\epsilon$ ), circumferential (SDT-c $\epsilon$ ) and radial (SDT-r $\epsilon$ ) directions, and the range of the six segments time to peak strain (RT- $\epsilon$ ) at longitudinal (RT-l $\epsilon$ ), circumferential (RT-c $\epsilon$ ) and radial (RT-r $\epsilon$ ) directions were also calculated.

Segmental heterogeneity (SH- $\epsilon$ ), defined as the range of the peak strain of the six segments, and transmural heterogeneity (TH-c $\epsilon$ ), defined as the difference of peak circumferential strain between endocardium and epicardium were also calculated.

### ***Statistical analysis***

All statistical analyses were performed with commercial computer static software (SPSS 12.0 Inc., Chicago, Illinois, USA). Data are express as the mean  $\pm$  standard deviation (SD).

Compare the strain, SR, SR<sub>E</sub> and SR<sub>A</sub> between six segments by one way-ANOVA and pairwise comparison by Scheffe's method as post-hoc analysis if variances agree to variance homogeneity test, if not, using Robust test (Brown-Forysthe test substitute for ANOVA) and Games-Howell method as post-hoc analysis. A 2-tailed  $P < 0.05$  was considered significant.

Spearman correlation was used to examine the linear association between continuous variables. A 2-tailed  $P < 0.05$  was considered significant.

## **Results**

The descriptive statistics of the indices derived from conventional echocardiography indices are listed in Table 1.

The intra-observer CV of 2D-STE variables are almost less than 25% except

RSR<sub>Ag</sub> was 25.39% (Table 2).

### **Myocardial strain and strain rate**

Based on the direction, values for circumferential and longitudinal peak systolic strain and strain rate were negative and values for radial peak systolic strain and peak systolic strain rate were positive for all cats (Table 3). Heterogeneity of strain and strain rate values across the 6 myocardial segments in the longitudinal analysis was found.

In general, circumferential, radial and longitudinal strain and strain rate were not affected by age, bodyweight, heart rate or blood pressure, except LSR<sub>Eg</sub> was negatively correlated with the heart rate ( $r=-0.591$ ,  $P=0.002$ , Table 4). Global circumferential ( $P=0.015$ ) and radial strain ( $P=0.018$ ) were lower in male.

### **Indices of 2D-STE and conventional echocardiography**

Either systolic or diastolic indices derive from B- or M-mode echocardiography was not correlated with indices of STE. The Vcf (FS/ET), derived from pw-Doppler and M-mode, was correlated with LSg ( $r=0.437$ ), LSRg ( $r=0.518$ ) and CSR<sub>Ag</sub> ( $r=0.524$ ), and AVp, also an index derived from pw-Doppler, was correlated with CSR<sub>Ag</sub> ( $r=0.478$ ), RSg ( $r=-0.432$ ), LSg ( $r=0.473$ ) and LSRg ( $r=0.454$ , Table 5).

The T<sub>E/A</sub> was correlated to CSRg ( $r=-0.440$ ), CSR<sub>Ag</sub> ( $r=-0.695$ ) and LSR<sub>Ag</sub> ( $r=-0.593$ ). The M<sub>E/A</sub> was correlated to LSg ( $r=-0.482$ ) and LSRg ( $r=-0.591$ ). In addition, MAVp was correlated to LSRg ( $r=0.434$ , Table 6).

### **Segmental heterogeneity and synchrony**

The segmental heterogeneity (SH- $\epsilon$ ) of SH-c $\epsilon$ , SH-r $\epsilon$  and SH-l $\epsilon$  was  $13.1 \pm 5.9\%$ ,  $19.1 \pm 10.3\%$ , and  $15.4 \pm 6.8\%$ , respectively. The TH-c $\epsilon$  was  $-14.3 \pm 4.6\%$  in circumferential direction (Table 7). The TH-c $\epsilon$  was correlated to body weight ( $r=-0.471$ ,  $P=0.027$ ) (Table 8).



The synchrony of SDT-cε, SDT-rε, and SDT-lε was  $11.7 \pm 4.2$  ms,  $16.5 \pm 13.4$  ms, and  $19.4 \pm 8.5$  ms, respectively; RT-cε, RT-rε, and RT-lε was  $32.5 \pm 9.3$  ms,  $40.2 \pm 28.7$  ms, and  $44.2 \pm 22.6$  ms, respectively (Table 7). The SDT-lε was correlated to heart rate ( $r=-0.433$ ,  $P=0.044$ , Table 8).

### **Segmental heterogeneity/synchrony and indices of conventional echocardiography**

Radial heterogeneity and synchrony were not correlated to systolic indices of conventional echocardiography. Circumferential transmural heterogeneity was well correlated to FAC ( $r=-0.841$ ,  $P<0.001$ ). Longitudinal synchrony (RT-lε, SDT-lε) were affected by AAT, AVp and AGp (Table 9).

Circumferential heterogeneity (SH-cε) was correlated to  $T_{E/A}$  ( $r=0.434$ ). Radial synchrony (RT-rε) was correlated to  $M_{E/A}$  ( $r=-0.470$ ). Longitudinal synchrony (RT-lε, SDT-lε) were correlated to IVRT ( $r=0.489$ ,  $r=0.461$ ) respectively (Table 10).

### **Segmental heterogeneity/synchrony and indices of 2D-STE**

Radial/longitudinal strain and strain rate were almost not correlated to synchrony. Heterogeneity (SH-cε, SH-lε) were correlated to CSg and LSg, respectively, and heterogeneity (TH-cε) was correlated to CSg ( $r=-0.817$ ,  $P<0.001$ ), CSRg ( $r=-0.816$ ,  $P<0.001$ ), and CSR<sub>Eg</sub> ( $r=-0.747$ ,  $P<0.001$ ) significantly (Table 11).

## **Discussion**

Left ventricular strain and strain rate have been reported to be significantly associated with various physical characteristics. In human patients left ventricular strain and strain rate are affected by heart rate, but also by age, gender and body weight [27-32]. The effects of physical status on Indices of strain and strain rate in dogs are less consistent. Myocardial strain and strain rate may not be affected age in

dogs [28], the effects of body weight and heart rate remains inconclusive [28, 33-35]. In this study, left ventricular strain and strain rate in cats were not affected by age, body weight, heart rate or blood pressure, except peak longitudinal early diastolic strain rate was affected by heart rate. A significant association between age and diastolic myocardial velocity was reported in cats [36]. However, the effect of age on myocardial motion remains controversial [36, 37]. In this study, gender appeared to affect myocardial strain. Based on these findings, the effects of physical characteristics on myocardial strain and strain rate should be taken into consideration, strain and strain rate might appear correlation with physiological factors if age or body weight range is expanded.

In general, cardiac systolic function is evaluated as contractility by pressure formation (PEP: ET and AAT derived from pulse-wave Doppler) or by deformation ( $EF_M$  and FS derived from M-mode) [38]. The mechanics of segmental myocardium (elasticity deformation) are complied wall stress and contractile force (Hooke's Law) [39]. Deformation of segmental myocardium cannot directly represent contractility, it is affected by wall stress (loading, overall cardiac volume changes), neighboring segments interaction (tension), cardiac geometry and elasticity (tissue properties).

The relationship between the left ventricular strain and the indices derived from conventional echocardiography (B- and M-mode) was weak and inconsistent in this study. It was not surprised that no significant association between the indices of 2D-STE and conventional echocardiography was found. Ventricular deformation is complemented in three directions. No single direction of the myocardial was assigned to a larger proportion of systolic function. Thus, conventional echocardiography is insensitive to detect regional dysfunction [40]. On the other hand, the  $EF_{ste}$  and FAC derived from 2D-STE are highly correlated to the estimated volume by MRI and

3D-STE in human patients [41]. In this study, correlation between  $EF_{ste}/FAC$  and myocardial strain were found in cats. Correlations between LS, LSR and  $M_{E/A}$ ,  $MAVp$  have also been reported in human patients [30]. Several systolic indices derived from pulse-wave Doppler were correlated to myocardial strain.

Based on these findings, both systolic and diastolic parameters derived from Doppler echocardiography might closely reflect systolic and diastolic strain rate. More cases with different cardiac conditions are needed to clarify the accuracy of the pressure gradient measured from Doppler echocardiography in association of myocardial strain rate.

### **Heterogeneity and synchrony**

In this study, both transmural and segmental heterogeneity of ventricle were demonstrated in clinically healthy cats. The characteristic of transmural heterogeneity of cats showed similar pattern of human subjects. The difference of  $TH-c\epsilon$  between endocardium and epicardium in this study was approximately 64% ( $TH-c\epsilon/Cg \times 100\%$ ) in contrast to 36% in human subjects [42]. And CS was decreasing from endocardium to epicardium, which also consistent with the pattern of human studies [42,43].

In this study, FAC was negatively correlated with  $TH-c\epsilon$ . The effect of transmural heterogeneity has to be taken consideration when FAC is changed. Heterogeneity of longitudinal direction was also found, significantly lower in the apex. Left ventricular heterogeneity in longitudinal direction has also been reported in human patients, however the pattern is inconsistent [27, 43-45].

In general, ventricular synchrony was not affected by age, body weight and strain, strain rate, heart rate, except  $SDT-l\epsilon$  was negatively associated with heart rate.  $SDT-l\epsilon$  and  $RT-l\epsilon$  were positively correlated to IVRT [46]. The intraventricular synchrony in

our studies was  $32.5 \pm 9.3$  ms in RT-ce,  $40.2 \pm 8.7$  ms in RT-re and  $44.2 \pm 22.6$  ms in RT-le, in contrast to value derived from in dogs with wide range of mean RT-re varied from 15 to 41.8 ms (SD varied from 2 to 17.9 ms) [28, 47, 48]. Although ventricular synchrony was not affected by strain in this study, the ranges for segmental intraventricular synchrony in clinically healthy cats were wide and the clinical application could be limited. However, the normal range of synchrony in cat was similar to dog and human, the possibility of species conservatives made application of synchrony with cut off value to diagnose or predict outcome of cardiac diseases implementable because human medicine have already used cut off value in resynchronization therapy field successfully.

## **Conclusion**

Longitudinal strain and strain rate was low in the segment of apex, CS decreasing from endocardium to epicardium. Left ventricular segmental and transmural heterogeneity was found in clinically healthy cats. Global myocardial strain and strain rate, heterogeneity and synchrony were nearly independent to age, body weight and heart rate.

## Reference

1. Yu C, Lin H, Zhang Q, Sanderson J: **High prevalence of left ventricular systolic and diastolic asynchrony in patients with congestive heart failure and normal QRS duration.** *Heart* 2003, **89**:54-60.
2. Hawkins NM, Petrie MC, MacDonald MR, Hogg KJ, McMurray JJ: **Selecting patients for cardiac resynchronization therapy: electrical or mechanical dyssynchrony?** *Eur Heart J* 2006, **27**:1270-1281.
3. Leclercq C, Faris O, Tunin R, Johnson J, Kato R, Evans F, Spinelli J, Halperin H, McVeigh E, Kass DA: **Systolic improvement and mechanical resynchronization does not require electrical synchrony in the dilated failing heart with left bundle-branch block.** *Circulation* 2002, **106**:1760-1763.
4. Kass DA: **Predicting cardiac resynchronization response by QRS duration: the long and short of it.** *J Am Coll Cardiol* 2003, **42**:2125-2127.
5. Fauchier L, Marie O, Casset-Senon D, Babuty D, Cosnay P, Fauchier JP: **Interventricular and intraventricular dyssynchrony in idiopathic dilated cardiomyopathy: a prognostic study with Fourier phase analysis of radionuclide angioscintigraphy.** *J Am Coll Cardiol* 2002, **40**:2022-2030.
6. Dohi K, Onishi K, Gorcsan III J, López-Candales A, Takamura T, Ota S, Yamada N, Ito M: **Role of radial strain and displacement imaging to quantify wall motion dyssynchrony in patients with left ventricular mechanical dyssynchrony and chronic right ventricular pressure overload.** *Am J Cardiol* 2008, **101**:1206-1212.
7. Soyama A, Kono T, Mishima T, Morita H, Ito T, Suwa M, Kitaura Y: **Intraventricular dyssynchrony may play a role in the development of mitral regurgitation in dilated cardiomyopathy.** *J Card Fail* 2005, **11**:631-637.
8. Spragg DD, Kass DA: **Pathobiology of left ventricular dyssynchrony and resynchronization.** *Prog Cardiovasc Dis* 2006, **49**:26-41.
9. Owen CH, Esposito DJ, Davis JW, Glower DD: **The effects of ventricular pacing on left ventricular geometry, function, myocardial oxygen consumption, and efficiency of contraction in conscious dogs.** *Pacing Clin Electrophysiol* 1998, **21**:1417-1429.
10. Bader H, Garrigue S, Lafitte S, Reuter S, Jaïs P, Haïssaguerre M, Bonnet J, Clementy J, Roudaut R: **Intra-left ventricular electromechanical asynchrony: a new independent predictor of severe cardiac events in heart failure patients.** *J Am Coll Cardiol* 2004, **43**:248-256.
11. Cho GY, Song JK, Park WJ, Han SW, Choi SH, Doo YC, Oh DJ, Lee Y:

- Mechanical dyssynchrony assessed by tissue Doppler imaging is a powerful predictor of mortality in congestive heart failure with normal QRS duration.** *J Am Coll Cardiol* 2005, **46**:2237-2243.
12. Thomas WP, Gaber CE, Jacobs GJ, Kaplan PM, Lombard CW, Moise N, Moses BL: **Recommendations for Standards in Transthoracic Two-Dimensional Echocardiography in the Dog and Cat.** *J Vet Intern Med* 1993, **7**:247-252.
  13. Troy BL, Pombo J, Rackley CE: **Measurement of left ventricular wall thickness and mass by echocardiography.** *Circulation* 1972, **45**:602-611.
  14. Lang RM, Bierig M, Devereux RB, Flachskampf FA, Foster E, Pellikka PA, Picard MH, Roman MJ, Seward J, Shanewise JS: **Recommendations for chamber quantification: a report from the American Society of Echocardiography's Guidelines and Standards Committee and the Chamber Quantification Writing Group, developed in conjunction with the European Association of Echocardiography, a branch of the European Society of Cardiology.** *J Am Soc Echocardiogr* 2005, **18**:1440-1463.
  15. Massie BM, Schiller NB, Ratshin RA, Parmley WW: **Mitral-septal separation: new echocardiographic index of left ventricular function.** *Am J Cardiol* 1977, **39**:1008-1016.
  16. Schwarz T, Johnson V: *BSAVA manual of canine and feline thoracic imaging*: Gloucester: British Small Animal Veterinary Association; 2008.
  17. Folland E, Parisi A, Moynihan P, Jones DR, Feldman C, Tow D: **Assessment of left ventricular ejection fraction and volumes by real-time, two-dimensional echocardiography. A comparison of cineangiographic and radionuclide techniques.** *Circulation* 1979, **60**:760-766.
  18. Sigurdardóttir L, Helgason H: **Echocardiographic evaluation of systolic and diastolic function in postoperative coarctation patients.** *Pediatr Cardiol* 1997, **18**:96-100.
  19. Burwash IG, Otto CM, Pearlman AS: **Use of Doppler-derived left ventricular time intervals for noninvasive assessment of systolic function.** *Am J Cardiol* 1993, **72**:1331-1333.
  20. Ben Zekry S, Saad RM, Ozkan M, Al Shahid MS, Pepi M, Muratori M, Xu J, Little SH, Zoghbi WA: **Flow acceleration time and ratio of acceleration time to ejection time for prosthetic aortic valve function.** *JACC Cardiovasc Imaging* 2011, **4**:1161-1170.
  21. Singer M, Allen MJ, Webb AR, Bennett ED: **Effects of alterations in left ventricular filling, contractility, and systemic vascular resistance on the ascending aortic blood velocity waveform of normal subjects.** *Crit Care*

- Med* 1991, **19**:1138-1145.
22. Lewis J, Kuo L, Nelson J, Limacher M, Quinones M: **Pulsed Doppler echocardiographic determination of stroke volume and cardiac output: clinical validation of two new methods using the apical window.** *Circulation* 1984, **70**:425-431.
  23. Borow KM, Green LH, Mann T, Sloss LJ, Braunwald E, Collins Jr JJ, Cohn L, Grossman W: **End-systolic volume as a predictor of postoperative left ventricular performance in volume overload from valvular regurgitation.** *Am J Med* 1980, **68**:655-663.
  24. Santilli RA, Bussadori C: **Doppler echocardiographic study of left ventricular diastole in non-anaesthetized healthy cats.** *Vet J* 1998, **156**:203-215.
  25. Tei C, Nishimura RA, Seward JB, Tajik AJ: **Noninvasive Doppler-derived myocardial performance index: correlation with simultaneous measurements of cardiac catheterization measurements.** *J Am Soc Echocardiogr* 1997, **10**:169-178.
  26. López-Alvarez J, Fonfara S, Pedro B, Stephenson H, Cripps PJ, Dukes-McEwan J: **Assessment of mechanical ventricular synchrony in Doberman Pinscher with dilated cardiomyopathy.** *J Vet Cardiol* 2011, **13**:183-195.
  27. Dalen H, Thorstensen A, Aase SA, Ingul CB, Torp H, Vatten LJ, Stoylen A: **Segmental and global longitudinal strain and strain rate based on echocardiography of 1266 healthy individuals: the HUNT study in Norway.** *Eur J Echocardiogr* 2010, **11**:176-183.
  28. Chetboul V, Serres F, Gouni V, Tissier R, Pouchelon JL: **Radial strain and strain rate by two-dimensional speckle tracking echocardiography and the tissue velocity based technique in the dog.** *J Vet Cardiol* 2007, **9**:69-81.
  29. Kuznetsova T, Herbots L, Richart T, D'hooge J, Thijs L, Fagard RH, Herregods MC, Staessen JA: **Left ventricular strain and strain rate in a general population.** *Eur Heart J* 2008, **29**:2014-2023.
  30. Lorch SM, Ludomirsky A, Singh GK: **Maturation and growth-related changes in left ventricular longitudinal strain and strain rate measured by two-dimensional speckle tracking echocardiography in healthy pediatric population.** *J Am Soc Echocardiogr* 2008, **21**:1207-1215.
  31. van Dalen BM, Soliman OII, Vletter WB, Folkert J, Geleijnse ML: **Age-related changes in the biomechanics of left ventricular twist measured by speckle tracking echocardiography.** *Am J Physiol Heart Circ Physiol* 2008, **295**:H1705-H1711.

32. Takeuchi M, Nakai H, Kokumai M, Nishikage T, Otani S, Lang RM: **Age-related changes in left ventricular twist assessed by two-dimensional speckle-tracking imaging.** *J Am Soc Echocardiogr* 2006, **19**:1077-1084.
33. Chetboul V, Gouni V, Sampedrano CC, Tissier R, Serres F, Pouchelon JL: **Assessment of regional systolic and diastolic myocardial function using tissue Doppler and strain imaging in dogs with dilated cardiomyopathy.** *J Vet Intern Med* 2007, **21**:719-730.
34. Simak J, Keller L, Killich M, Hartmann K, Wess G: **Color-coded longitudinal interventricular septal tissue velocity imaging, strain and strain rate in healthy Doberman Pinschers.** *J Vet Cardiol* 2011, **13**:1-11.
35. Smith DN, Bonagura JD, Culwell NM, Schober KE: **Left ventricular function quantified by myocardial strain imaging in small-breed dogs with chronic mitral regurgitation.** *J Vet Cardiol* 2012, **14**:231-242.
36. Simpson KE, Gunn-Moore DA, Shaw DJ, French AT, Dukes-McEwan J, Moran CM, Corcoran BM: **Pulsed-wave Doppler tissue imaging velocities in normal geriatric cats and geriatric cats with primary or systemic diseases linked to specific cardiomyopathies in humans, and the influence of age and heart rate upon these velocities.** *J Feline Med Surg* 2009, **11**:293-304.
37. Koffas H, Dukes-McEwan J, Corcoran B, Moran C, French A, Sboros V, Anderson T, Smith P, Simpson K, McDicken W: **Peak Mean Myocardial Velocities and Velocity Gradients Measured by Color M-Mode Tissue Doppler Imaging in Healthy Cats.** *J Vet Intern Med* 2003, **17**:510-524.
38. Kass D, Maughan W, Guo ZM, Kono A, Sunagawa K, Sagawa K: **Comparative influence of load versus inotropic states on indexes of ventricular contractility: experimental and theoretical analysis based on pressure-volume relationships.** *Circulation* 1987, **76**:1422-1436.
39. Bijnsens BH, Cikes M, Claus P, Sutherland GR: **Velocity and deformation imaging for the assessment of myocardial dysfunction.** *Eur J Echocardiogr* 2009, **10**:216-226.
40. Edvardsen T, Helle-Valle T, Smiseth OA: **Systolic dysfunction in heart failure with normal ejection fraction: speckle-tracking echocardiography.** *Prog Cardiovasc Dis* 2006, **49**:207-214.
41. Nishikage T, Nakai H, Mor-Avi V, Lang RM, Salgo IS, Settlemier SH, Husson S, Takeuchi M: **Quantitative assessment of left ventricular volume and ejection fraction using two-dimensional speckle tracking echocardiography.** *Eur J Echocardiogr* 2009, **10**:82-88.
42. Adamu U, Schmitz F, Becker M, Kelm M, Hoffmann R: **Advanced speckle**



- tracking echocardiography allowing a three-myocardial layer-specific analysis of deformation parameters.** *Eur J Echocardiogr* 2009, **10**:303-308.
43. Leitman M, Lysiansky M, Lysyansky P, Friedman Z, Tyomkin V, Fuchs T, Adam D, Krakover R, Vered Z: **Circumferential and longitudinal strain in 3 myocardial layers in normal subjects and in patients with regional left ventricular dysfunction.** *J Am Soc Echocardiogr* 2010, **23**:64-70.
44. Marwick TH, Leano RL, Brown J, Sun JP, Hoffmann R, Lysyansky P, Becker M, Thomas JD: **Myocardial strain measurement with 2-dimensional speckle-tracking echocardiography: definition of normal range.** *JACC Cardiovasc Imaging* 2009, **2**:80-84.
45. Amundsen BH, Crosby J, Steen PA, Torp H, Slordahl SA, Stoylen A: **Regional myocardial long-axis strain and strain rate measured by different tissue Doppler and speckle tracking echocardiography methods: a comparison with tagged magnetic resonance imaging.** *Eur J Echocardiogr* 2009, **10**:229-237.
46. Ng AC, Tran DT, Newman M, Allman C, Vidaic J, Lo ST, Hopkins AP, Leung DY: **Left ventricular longitudinal and radial synchrony and their determinants in healthy subjects.** *J Am Soc Echocardiogr* 2008, **21**:1042-1048.
47. Takano H, Fujii Y, Ishikawa R, Aoki T, Wakao Y: **Comparison of left ventricular contraction profiles among small, medium, and large dogs by use of two-dimensional speckle-tracking echocardiography.** *Am J Vet Res* 2010, **71**:421-427.
48. Griffiths LG, Fransioli JR, Chigerwe M: **Echocardiographic assessment of interventricular and intraventricular mechanical synchrony in normal dogs.** *J Vet Cardiol* 2011, **13**:115-126.

**Table 1.** The descriptive statistics of the population characteristic and conventional echocardiography indices of 34 clinically healthy cats

Parameter	Value
Age (years)	3.11 ± 2.17
Body weight (kg)	4.32 ± 1.32
sex	Male: n=18 (52.9%) Female: n=16 (47.1%)
Heart rate (beats/min)	171.97 ± 27.23
Systemic blood pressure (mmHg)	119.47 ± 15.15
IVSd (mm)	4.08 ± 0.61
LVFWd (mm)	4.17 ± 0.65
LVDd (mm)	14.98 ± 1.63
LVDs (mm)	6.81 ± 1.58
LA/Ao	1.35 ± 0.16
LVMI (g/m <sup>2</sup> )	28.53 ± 7.31
EPSS (mm)	0.43 ± 0.25
IVS% (%)	69.66 ± 17.84
LVFW% (%)	63.19 ± 15.24
FS (%)	54.74 ± 8.01
EF <sub>M</sub> (%)	87.24 ± 6.53
Vcf (circumferences/s)	0.38 ± 0.07
PEP:ET	0.29 ± 0.08
AAT (ms)	25.53 ± 7.74
AVp (m/s)	0.95 ± 0.20
AGp (mmHg)	1.12 ± 0.43
PVp (m/s)	0.90 ± 0.18
SV (ml)	354.1 ± 97.93
ESVI (ml/m <sup>2</sup> )	5.11 ± 1.96
MEVp (m/s)	0.82 ± 0.14
MAVp (m/s)	0.68 ± 0.16
M <sub>E/A</sub>	1.25 ± 0.27
TEVp (m/s)	0.65 ± 0.15
TAVp (m/s)	0.52 ± 0.14
T <sub>E/A</sub>	1.29 ± 0.27
IVRT (ms)	44.17 ± 7.42
Tei index	0.51 ± 0.09
Q <sub>P-Ao</sub> (ms)	-3.90 ± 13.22

AAT: aortic outflow acceleration time, AGp: aortic outflow peak velocity pressure gradient, AVp: aortic outflow peak velocity,  $EF_M$ : ejection fraction derived from m-mode, EPSS: E point to septal separation, ESVI: end systolic volume index, FS: fractional shortening, IVRT: isovolumic relaxation time, IVS%: percentage thickening of the interventricular septum, IVSd: interventricular septum thickness in end-diastole, LA/Ao: the ratio of left atrium and aortic diameter, LVDd: left ventricular dimension in end-diastole, LVDs: left ventricular dimension in end-systole, LVFW%: percentage thickening of the left ventricular free wall, LVFWd: left ventricular free wall thickness in end-diastole, LVMI: left ventricular mass index, MAVp: peak late mitral inflow velocity,  $M_{E/A}$ : early and late mitral inflow ratio, MEVp: peak early mitral inflow velocity, PEP:ET: pre-ejection time period and ejection time ratio, PVp: pulmonary outflow peak velocity,  $Q_{P-Ao}$ : difference between pulmonary pre-ejection time and aortic pre-ejection time, SV: stroke volume, TAVp: peak late tricuspid inflow velocity,  $T_{E/A}$ : early and late tricuspid inflow ratio, Tei index: myocardial performance index, TEVp: peak early tricuspid inflow velocity, Vcf: velocity of circumferential fiber shortening.



**Table 2.** The intra-observer coefficient of variance (CV) of 2D-STE variables

	Intra-observer CV (%)		Intra-observer CV (%)		Intra-observer CV (%)
CSg	6.43	RSg	10.24	LSg	4.56
CSRg	5.92	RSRg	14.91	LSRg	9.16
CSR <sub>Eg</sub>	12.37	RSR <sub>Eg</sub>	9.55	LSR <sub>Eg</sub>	21.08
CSR <sub>Ag</sub>	18.58	RSR <sub>Ag</sub>	25.39	LSR <sub>Ag</sub>	12.26

CSg: global peak circumferential strain, CSR<sub>Ag</sub>: global peak circumferential late diastolic strain rate, CSR<sub>Eg</sub>: global peak circumferential early diastolic strain rate, CSRg: global peak circumferential systolic strain rate, LSg: global peak longitudinal strain, LSR<sub>Ag</sub>: global peak longitudinal late diastolic strain rate, LSR<sub>Eg</sub>: global peak longitudinal early diastolic strain rate, LSRg: global peak longitudinal systolic strain rate, RSg: global peak radial strain, RSR<sub>Ag</sub>: global peak radial late diastolic strain rate, RSR<sub>Eg</sub>: global peak radial early diastolic strain rate, RSRg: global peak radial systolic strain rate.

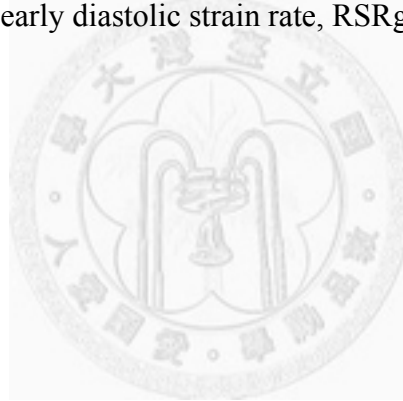


**Table 3.** Circumferential, radial and longitudinal strain and systolic strain rate values for regional left ventricular segments determined using two-dimensional speckle tracking echocardiography in 34 clinical healthy cats

CS (%)		CSR (s <sup>-1</sup> )		RS (%)		RSR (s <sup>-1</sup> )		LS (%)		LSR (s <sup>-1</sup> )	
CS <sub>1</sub>	-21.87 ± 6.69	CSR <sub>1</sub>	-2.60 ± 0.78	RS <sub>1</sub>	26.32 ± 11.64	RSR <sub>1</sub>	2.40 ± 0.82	LS <sub>1</sub>	-18.69 ± 4.92	LSR <sub>1</sub>	-2.23 ± 0.70
CS <sub>2</sub>	-21.83 ± 6.40	CSR <sub>2</sub>	-2.73 ± 0.97	RS <sub>2</sub>	25.50 ± 13.58	RSR <sub>2</sub>	2.38 ± 1.02	LS <sub>2</sub>	-18.85 ± 4.46	LSR <sub>2</sub>	-2.33 ± 0.59
CS <sub>3</sub>	-21.82 ± 5.97	CSR <sub>3</sub>	-2.77 ± 0.95	RS <sub>3</sub>	27.12 ± 12.76	RSR <sub>3</sub>	2.46 ± 0.95	LS <sub>3</sub>	-15.36 ± 6.30	LSR <sub>3</sub>	-1.87 ± 0.84†
CS <sub>4</sub>	-21.98 ± 7.81	CSR <sub>4</sub>	-2.75 ± 1.21	RS <sub>4</sub>	27.38 ± 10.36	RSR <sub>4</sub>	2.43 ± 0.84	LS <sub>4</sub>	-13.67 ± 5.37*	LSR <sub>4</sub>	-1.63 ± 0.66*
CS <sub>5</sub>	-21.90 ± 8.52	CSR <sub>5</sub>	-2.73 ± 1.17	RS <sub>5</sub>	28.68 ± 10.04	RSR <sub>5</sub>	2.67 ± 1.00	LS <sub>5</sub>	-19.84 ± 8.00	LSR <sub>5</sub>	-2.42 ± 1.00
CS <sub>6</sub>	-23.03 ± 7.15	CSR <sub>6</sub>	-2.61 ± 0.87	RS <sub>6</sub>	29.46 ± 12.71	RSR <sub>6</sub>	2.74 ± 1.00	LS <sub>6</sub>	-22.93 ± 10.80	LSR <sub>6</sub>	-2.80 ± 1.24
CS <sub>g</sub>	-22.26 ± 5.01	CSR <sub>g</sub>	-2.7 ± 0.72	RS <sub>g</sub>	26.08 ± 8.18	RSR <sub>g</sub>	2.51 ± 0.71	LS <sub>g</sub>	-18.22 ± 4.78	LSR <sub>g</sub>	-2.21 ± 0.58
ANOVA	P=0.997		P=0.996		P=0.913		P=0.793		P<0.001		P<0.001
CSR <sub>E</sub> (s <sup>-1</sup> )		CSR <sub>A</sub> (s <sup>-1</sup> )		RSR <sub>E</sub> (s <sup>-1</sup> )		RSR <sub>A</sub> (s <sup>-1</sup> )		LSR <sub>E</sub> (s <sup>-1</sup> )		LSR <sub>A</sub> (s <sup>-1</sup> )	
CSR <sub>E1</sub>	2.71 ± 1.33	CSR <sub>A1</sub>	0.99 ± 0.38	RSR <sub>E1</sub>	-2.18 ± 1.59	RSR <sub>A1</sub>	-1.62 ± 0.93	LSR <sub>E1</sub>	1.88 ± 0.81	LSR <sub>A1</sub>	1.55 ± 0.98
CSR <sub>E2</sub>	2.33 ± 1.09	CSR <sub>A2</sub>	0.99 ± 0.23	RSR <sub>E2</sub>	-2.09 ± 1.20	RSR <sub>A2</sub>	-1.55 ± 0.82	LSR <sub>E2</sub>	1.89 ± 0.65	LSR <sub>A2</sub>	1.45 ± 0.45
CSR <sub>E3</sub>	2.35 ± 1.00	CSR <sub>A3</sub>	1.13 ± 0.51	RSR <sub>E3</sub>	-2.28 ± 1.06	RSR <sub>A3</sub>	-1.69 ± 0.93	LSR <sub>E3</sub>	1.55 ± 0.81	LSR <sub>A3</sub>	0.92 ± 0.52
CSR <sub>E4</sub>	2.22 ± 1.41	CSR <sub>A4</sub>	1.15 ± 0.74	RSR <sub>E4</sub>	-1.89 ± 1.01	RSR <sub>A4</sub>	-1.70 ± 0.90	LSR <sub>E4</sub>	1.29 ± 0.82	LSR <sub>A4</sub>	0.93 ± 0.55
CSR <sub>E5</sub>	2.33 ± 1.39	CSR <sub>A5</sub>	1.33 ± 0.63	RSR <sub>E5</sub>	-1.92 ± 1.26	RSR <sub>A5</sub>	-1.80 ± 0.88	LSR <sub>E5</sub>	1.78 ± 1.12	LSR <sub>A5</sub>	1.28 ± 0.94
CSR <sub>E6</sub>	2.53 ± 0.91	CSR <sub>A6</sub>	1.21 ± 0.48	RSR <sub>E6</sub>	-2.06 ± 1.56	RSR <sub>A6</sub>	-1.92 ± 1.10	LSR <sub>E6</sub>	1.80 ± 1.37	LSR <sub>A6</sub>	1.42 ± 1.16
CSR <sub>Eg</sub>	2.39 ± 0.81	CSR <sub>Ag</sub>	1.16 ± 0.32	RSR <sub>Eg</sub>	-1.99 ± 1.12	RSR <sub>Ag</sub>	-1.82 ± 0.85	LSR <sub>Eg</sub>	1.52 ± 0.73	LSR <sub>Ag</sub>	1.21 ± 0.57
ANOVA	P=0.920		P=0.536		P=0.980		P=0.930		P=0.664		P=0.393

C<sub>1</sub>: cranio-septal, C<sub>2</sub>: cranial, C<sub>3</sub>: lateral, C<sub>4</sub>: caudal, C<sub>5</sub>: ventral, C<sub>6</sub>: septal, C<sub>g</sub>: global, CS: peak circumferential strain, CSR: peak circumferential strain rate, CSR<sub>A</sub>: peak circumferential late diastolic strain rate, CSR<sub>E</sub>: peak circumferential early diastolic strain rate, L<sub>1</sub>: basal septa, L<sub>2</sub>: mid septal, L<sub>3</sub>: apical septal, L<sub>4</sub>: apical lateral, L<sub>5</sub>: mid lateral, L<sub>6</sub>: basal lateral, L<sub>g</sub>: global, LS: peak longitudinal strain, LSR: peak longitudinal strain rate, LSR<sub>A</sub>: peak longitudinal late diastolic strain rate, LSR<sub>E</sub>: peak longitudinal early diastolic strain rate, R<sub>1</sub>: cranio-septal, R<sub>2</sub>: cranial, R<sub>3</sub>: lateral, R<sub>4</sub>: caudal, R<sub>5</sub>: ventral, R<sub>6</sub>: septal, R<sub>g</sub>: global, RS: peak radial strain, RSR: peak radial strain rate, RSR<sub>A</sub>: peak radial late diastolic strain rate, RSR<sub>E</sub>: peak radial early diastolic strain rate.

\*LS/LSR<sub>1,2,5,6,g</sub> were different from LS<sub>4</sub> significantly ( $P<0.05$ ) and †LSR<sub>3</sub> was significantly different from LS<sub>6</sub> in post hoc pairwise comparison by Game's-Howell.

**Table 4.** Characteristics of cats and indices of strain and strain rate

	Age		Body weight		Heart rate		Blood pressure	
	<i>r</i>	<i>P</i>	<i>r</i>	<i>P</i>	<i>r</i>	<i>P</i>	<i>r</i>	<i>P</i>
CSg	0.125	0.580	0.133	0.556	-0.076	0.736	0.060	0.801
CSRg	0.182	0.418	0.248	0.266	0.211	0.346	-0.029	0.905
CSR <sub>Eg</sub>	0.015	0.948	0.347	0.123	0.157	0.496	0.008	0.974
CSR <sub>Ag</sub>	-0.245	0.284	0.146	0.529	0.398	0.074	-0.299	0.214
RSg	-0.096	0.672	-0.014	0.952	-0.302	0.172	-0.409	0.073
RSRg	0.050	0.826	0.225	0.313	-0.017	0.941	-0.377	0.101
RSR <sub>Eg</sub>	0.068	0.777	0.388	0.091	-0.187	0.429	0.034	0.893
RSR <sub>Ag</sub>	-0.002	0.992	0.172	0.470	0.309	0.184	-0.285	0.251
LSg	0.189	0.365	-0.078	0.718	-0.064	0.760	0.020	0.926
LSRg	0.227	0.276	-0.094	0.662	0.060	0.776	-0.014	0.949
LSR <sub>Eg</sub>	-0.094	0.739	0.077	0.785	-0.591	0.020*	0.021	0.943
LSR <sub>Ag</sub>	0.312	0.278	-0.013	0.964	0.200	0.493	0.314	0.297

CSg: global peak circumferential strain, CSR<sub>Ag</sub>: global peak circumferential late diastolic strain rate, CSR<sub>Eg</sub>: global peak circumferential early diastolic strain rate, CSRg: global peak circumferential systolic strain rate, LSg: global peak longitudinal strain, LSR<sub>Ag</sub>: global peak longitudinal late diastolic strain rate, LSR<sub>Eg</sub>: global peak longitudinal early diastolic strain rate, LSRg: global peak longitudinal strain rate, RSg: global peak radial strain, RSR<sub>Ag</sub>: global peak radial late diastolic strain rate, RSR<sub>Eg</sub>: global peak radial early diastolic strain rate, RSRg: global peak radial systolic strain rate.

*r*=Spearman correlation coefficient, \**P*<0.05 (two tail), significant correlation.

**Table 5.** Relationship between indices derived from conventional echocardiography and strain and strain rate

		LVMI	EPSS	IVS%	LVFW%	FS	EF <sub>M</sub>	Vcf	PEP:ET	AAT	AVp	AGp	PVp	SV	ESVI	FAC
CSg	<i>r</i>	0.206	-0.152	0.049	0.110	0.206	0.175	0.086	0.191	-0.294	0.233	-0.101	0.056	0.235	0.200	0.937
	<i>P</i>	0.371	0.499	0.832	0.634	0.357	0.437	0.711	0.408	0.196	0.296	0.662	0.805	0.305	0.411	0.000*
CSRg	<i>r</i>	0.014	-0.340	0.005	0.162	0.29	0.272	0.254	0.031	-0.387	0.386	0.087	0.174	0.148	0.294	0.874
	<i>P</i>	0.953	0.121	0.982	0.482	0.190	0.221	0.267	0.893	0.083	0.076	0.709	0.440	0.522	0.222	0.000*
CSR <sub>Eg</sub>	<i>r</i>	-0.036	-0.342	0.079	0.060	0.128	0.117	0.075	0.117	-0.225	0.192	-0.024	0.323	0.033	0.228	0.635
	<i>P</i>	0.880	0.129	0.741	0.801	0.58	0.613	0.754	0.622	0.340	0.405	0.920	0.154	0.890	0.363	0.002*
CSR <sub>Ag</sub>	<i>r</i>	0.029	-0.336	0.191	0.289	0.28	0.314	0.524	-0.213	-0.307	0.478	0.319	0.250	0.280	0.346	0.361
	<i>P</i>	0.905	0.137	0.420	0.217	0.219	0.166	0.018*	0.367	0.188	0.028*	0.171	0.275	0.232	0.160	0.108
RSg	<i>r</i>	0.242	0.096	0.372	0.042	0.292	0.234	0.104	0.217	0.134	-0.432	-0.338	-0.181	0.139	0.242	0.562
	<i>P</i>	0.290	0.670	0.097	0.858	0.187	0.294	0.655	0.344	0.564	0.044*	0.134	0.420	0.548	0.318	0.007*
RSRg	<i>r</i>	0.146	-0.076	0.258	0.205	0.374	0.351	0.396	0.205	-0.098	-0.198	-0.127	0.201	-0.031	0.116	0.513
	<i>P</i>	0.527	0.738	0.259	0.374	0.086	0.109	0.076	0.374	0.672	0.377	0.585	0.369	0.895	0.637	0.015*
RSR <sub>Eg</sub>	<i>r</i>	0.049	-0.123	0.075	-0.037	-0.001	-0.032	0.135	0.326	0.056	-0.136	-0.451	-0.140	-0.284	-0.336	0.307
	<i>P</i>	0.842	0.607	0.762	0.881	0.997	0.892	0.583	0.173	0.819	0.567	0.053	0.556	0.238	0.187	0.188
RSR <sub>Ag</sub>	<i>r</i>	0.006	0.221	-0.134	0.432	0.288	0.264	0.401	-0.101	-0.100	0.026	0.366	0.367	0.232	0.416	0.409
	<i>P</i>	0.980	0.349	0.584	0.065	0.218	0.260	0.089	0.681	0.682	0.912	0.124	0.111	0.340	0.097	0.073
LSg	<i>r</i>	-0.231	-0.047	-0.136	0.057	0.236	0.145	0.437	-0.006	-0.059	0.473	0.104	0.212	0.079	-0.258	0.713
	<i>P</i>	0.277	0.823	0.526	0.790	0.257	0.490	0.037*	0.979	0.784	0.020*	0.630	0.310	0.713	0.224	0.000*
LSRg	<i>r</i>	-0.302	-0.026	-0.094	0.123	0.276	0.171	0.518	-0.038	-0.195	0.454	0.128	0.346	0.060	-0.361	0.719
	<i>P</i>	0.152	0.904	0.662	0.568	0.182	0.414	0.011*	0.859	0.362	0.026*	0.552	0.090	0.781	0.083	0.000*
LSR <sub>Eg</sub>	<i>r</i>	0.064	0.113	-0.416	-0.345	-0.136	-0.199	-0.248	0.269	0.363	0.176	-0.179	-0.182	0.101	0.154	0.484
	<i>P</i>	0.820	0.688	0.139	0.226	0.629	0.478	0.414	0.353	0.202	0.547	0.540	0.515	0.731	0.584	0.067
LSR <sub>Ag</sub>	<i>r</i>	-0.297	0.005	-0.154	0.478	0.411	0.453	0.543	-0.017	-0.327	0.495	0.124	0.469	-0.132	-0.600	0.420
	<i>P</i>	0.303	0.988	0.616	0.098	0.144	0.104	0.068	0.957	0.275	0.085	0.685	0.091	0.668	0.023*	0.135

AAT: aortic outflow acceleration time, AGp: aortic outflow peak velocity pressure gradient, AVp: aortic outflow peak velocity, CSg: global peak circumferential strain, CSRg: global peak circumferential systolic strain rate, CSR<sub>Ag</sub>: global peak circumferential late diastolic strain rate, CSR<sub>Eg</sub>: global peak circumferential early diastolic strain rate, EF<sub>M</sub>: ejection fraction derived from m-mode, EPSS: E point to septal separation, ESVI: end systolic volume index, FAC: fractional area change, FS: fractional shortening, IVS%: percentage thickening of the interventricular septum, LSg: global peak longitudinal strain, LSRg: global peak longitudinal systolic strain rate, LSR<sub>Ag</sub>: global peak longitudinal late diastolic strain rate, LSR<sub>E</sub>: longitudinal early diastolic strain rate, LVFW%: percentage thickening of the left ventricular free wall, LVMI: left ventricular mass index, PEP:ET: pre-ejection time period and ejection time ratio, PVp: pulmonary outflow peak velocity, SV: stroke volume, RSg: global peak radial strain, RSRg: global peak radial systolic strain rate, RSR<sub>Ag</sub>: global peak radial late diastolic strain rate, RSR<sub>Eg</sub>: global peak radial early diastolic strain rate, Vcf: velocity of circumferential fiber shortening.

$r$ =Spearman correlation coefficient, \* $P < 0.05$  (two tail), significant correlation.

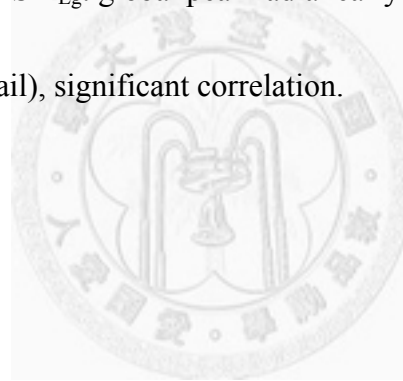




**Table 6.** Relationship between indices derived from Doppler echocardiography and strain and strain rate

		MEVp	MAVp	M <sub>E/A</sub>	TEVp	TAVp	T <sub>E/A</sub>	IVRT	Tei index
CSg	<i>r</i>	0.186	0.123	0.034	0.027	0.144	-0.258	0.124	0.068
	<i>P</i>	0.407	0.584	0.879	0.906	0.533	0.259	0.614	0.781
CSRg	<i>r</i>	0.355	0.309	-0.072	0.170	0.370	-0.440	0.140	0.262
	<i>P</i>	0.105	0.162	0.749	0.460	0.099	0.046*	0.569	0.279
CSR <sub>Eg</sub>	<i>r</i>	0.243	0.110	-0.019	0.248	0.316	-0.165	0.045	0.135
	<i>P</i>	0.289	0.635	0.935	0.291	0.174	0.488	0.858	0.592
CSR <sub>Ag</sub>	<i>r</i>	0.317	0.084	0.053	-0.081	0.330	-0.695	0.332	0.313
	<i>P</i>	0.162	0.717	0.821	0.733	0.155	0.001*	0.179	0.206
RSg	<i>r</i>	-0.041	-0.286	0.375	0.004	-0.028	0.079	0.024	-0.196
	<i>P</i>	0.857	0.196	0.086	0.987	0.904	0.733	0.923	0.422
RSRg	<i>r</i>	0.176	-0.117	0.372	0.073	0.231	-0.259	0.000	-0.051
	<i>P</i>	0.432	0.603	0.089	0.752	0.314	0.257	1.000	0.836
RSR <sub>Eg</sub>	<i>r</i>	0.114	-0.062	0.243	-0.04	0.267	-0.193	-0.093	-0.061
	<i>P</i>	0.633	0.796	0.302	0.869	0.269	0.428	0.714	0.810
RSR <sub>Ag</sub>	<i>r</i>	0.378	0.268	-0.096	0.302	0.389	-0.397	-0.157	-0.262
	<i>P</i>	0.100	0.253	0.686	0.208	0.100	0.093	0.534	0.293
LSg	<i>r</i>	0.108	0.374	-0.482	0.046	0.182	-0.252	0.189	0.250
	<i>P</i>	0.608	0.066	0.015*	0.826	0.384	0.224	0.411	0.275
LSRg	<i>r</i>	0.060	0.434	-0.591	0.074	0.204	-0.288	0.161	0.249
	<i>P</i>	0.775	0.030*	0.002*	0.726	0.329	0.163	0.486	0.277
LSR <sub>Eg</sub>	<i>r</i>	0.044	0.059	-0.152	-0.170	-0.203	0.000	0.182	0.056
	<i>P</i>	0.876	0.834	0.589	0.544	0.468	1.000	0.570	0.862
LSR <sub>Ag</sub>	<i>r</i>	-0.212	0.301	-0.414	-0.046	0.499	-0.593	0.132	0.246
	<i>P</i>	0.468	0.296	0.142	0.875	0.069	0.026*	0.699	0.466

CSg: global peak circumferential strain, CSRg: global peak circumferential systolic strain rate, CSR<sub>Ag</sub>: global peak circumferential late diastolic strain rate, CSR<sub>Eg</sub>: global peak circumferential early diastolic strain rate, IVRT: isovolumic relaxation time, LSg: global peak longitudinal strain, LSRg: global peak longitudinal systolic strain rate, LSR<sub>Ag</sub>: global peak longitudinal late diastolic strain rate, LSR<sub>Eg</sub>: global peak longitudinal early diastolic strain rate, MAVp: peak late mitral inflow velocity, M<sub>E/A</sub>: early and late mitral inflow ratio, MEVp: peak early mitral inflow velocity, RSg: global peak radial strain, RSRg: global peak radial systolic strain rate, RSR<sub>Ag</sub>: global peak radial late diastolic strain rate, RSR<sub>Eg</sub>: global peak radial early diastolic strain rate, TAVp: peak late tricuspid inflow velocity, T<sub>E/A</sub>: early and late tricuspid inflow ratio, Tei index: myocardial performance index, TEVp: peak early tricuspid inflow velocity.

$r$ =Spearman correlation coefficient, \* $P$ <0.05 (two tail), significant correlation.

**Table 7.** Descriptive statistics of ventricular heterogeneity and synchrony in clinically healthy cats

Circumference		Radiation		Longitude	
RT-cε (ms)	32.49 ± 9.32	RT-rε (ms)	40.21 ± 28.72	RT-lε (ms)	44.24 ± 22.62
SDT-cε (ms)	11.74 ± 4.16	SDT-rε (ms)	16.48 ± 13.41	SDT-lε (ms)	19.38 ± 8.52
SH-cε (%)	13.05 ± 5.86	SH-rε (%)	19.06 ± 10.34	SH-lε (%)	15.38 ± 6.81
TH-cε (%)	-14.28 ± 4.60				

Q<sub>P-Ao</sub>: -3.9 ± 13.22 ms

Q<sub>P-Ao</sub>: difference between pulmonary pre-ejection time and aortic pre-ejection time, RT-cε: range of the 6 segment time to peak circumferential strain, RT-rε: range of the 6 segment time to peak radial strain, RT-lε: range of the 6 segment time to peak longitudinal strain, SDT-cε: standard deviation of the 6 segment time to peak circumferential strain, SDT-rε: standard deviation of the 6 segment time to peak radial strain, SDT-lε: standard deviation of the 6 segment time to peak longitudinal strain, SH-cε: circumferential segmental heterogeneity, SH-rε: radial segmental heterogeneity, SH-lε: longitudinal segmental heterogeneity, TH-cε: circumferential transmural heterogeneity.

**Table 8.** Characteristics of cats and ventricular synchrony (RT-ε, SDT-ε) and heterogeneity (SH-ε, TH-cε)

	Age		Body weight		Heart rate		Blood pressure	
	$r$	$P$	$r$	$P$	$r$	$P$	$r$	$P$
RT-cε	0.168	0.455	0.012	0.957	-0.05	0.824	-0.005	0.982
SDT-cε	0.244	0.274	-0.038	0.867	-0.011	0.962	-0.008	0.975
SH-cε	0.161	0.475	0.246	0.269	0.102	0.65	0.121	0.611
TH-cε	-0.175	0.436	-0.471	0.027*	-0.137	0.542	-0.151	0.524
RT-rε	0.025	0.914	0.058	0.799	0.221	0.322	-0.072	0.764
SDT-rε	0.015	0.949	0.046	0.838	0.124	0.584	-0.052	0.828
SH-rε	0.095	0.675	-0.249	0.265	-0.221	0.323	-0.079	0.740
RT-lε	0.214	0.316	0.027	0.901	-0.273	0.197	0.136	0.538
SDT-lε	0.280	0.207	0.123	0.594	-0.433	0.044*	0.197	0.393
SH-lε	-0.235	0.258	-0.208	0.329	-0.246	0.235	-0.071	0.743
Q <sub>P-Ao</sub>	0.185	0.376	-0.320	0.119	-0.319	0.138	0.227	0.298

Q<sub>P-Ao</sub>: difference between pulmonary pre-ejection time and aortic pre-ejection time, RT-cε: range of time to peak circumferential strain, RT-lε: range of time to peak longitudinal strain, RT-rε: range of time to peak radial strain, SDT-cε: standard deviation of time to peak circumferential strain, SDT-lε: standard deviation of time to peak longitudinal strain, SDT-rε: standard deviation of time to peak radial strain, SH-cε: segmental heterogeneity in circumferential strain, SH-lε: segmental heterogeneity in longitudinal strain, SH-rε: segmental heterogeneity in radial strain, TH-cε: transmural heterogeneity in circumferential strain, \* $P$ <0.05 (two tail), correlation significant,  $r$ =Spearman correlation coefficient.

**Table 9.** Relationship between indices derived from conventional echocardiography and left ventricular synchrony and heterogeneity

		LVMI	EPSS	IVS%	LVFW%	FS	EF <sub>M</sub>	Vcf	PEP:ET	AAT	AVp	AGp	PVp	SV	ESVI	FAC
RT-cε	<i>r</i>	-0.096	0.257	0.075	0.267	0.195	0.202	0.200	-0.139	0.236	-0.213	-0.179	0.360	0.089	-0.297	-0.266
	<i>P</i>	0.680	0.248	0.747	0.242	0.383	0.368	0.385	0.548	0.303	0.342	0.437	0.100	0.701	0.216	0.231
SDT-cε	<i>r</i>	-0.030	0.144	0.043	0.275	0.172	0.190	0.230	-0.034	0.096	-0.083	-0.095	0.339	0.003	-0.133	-0.216
	<i>P</i>	0.898	0.523	0.854	0.228	0.444	0.398	0.316	0.884	0.679	0.712	0.681	0.123	0.989	0.588	0.334
SH-cε	<i>r</i>	-0.118	-0.029	-0.112	-0.004	0.058	0.040	0.187	-0.072	-0.334	0.240	-0.048	0.097	-0.255	-0.144	0.308
	<i>P</i>	0.612	0.900	0.628	0.987	0.799	0.859	0.417	0.758	0.139	0.283	0.836	0.669	0.265	0.557	0.164
TH-cε	<i>r</i>	0.149	0.378	-0.160	-0.083	-0.296	-0.282	-0.209	-0.248	0.264	-0.190	0.239	-0.063	-0.006	-0.044	-0.841
	<i>P</i>	0.518	0.083	0.487	0.720	0.182	0.203	0.364	0.279	0.247	0.397	0.297	0.779	0.978	0.858	0.000*
RT-rε	<i>r</i>	-0.137	0.163	-0.348	-0.112	-0.076	-0.038	0.045	-0.382	0.012	0.215	0.416	0.157	0.114	0.211	0.027
	<i>P</i>	0.552	0.468	0.122	0.630	0.736	0.867	0.845	0.087	0.959	0.335	0.061	0.485	0.624	0.386	0.907
SDT-rε	<i>r</i>	-0.067	0.230	-0.380	-0.144	-0.110	-0.072	0.020	-0.300	0.016	0.187	0.363	0.132	0.120	0.132	0.097
	<i>P</i>	0.773	0.303	0.089	0.535	0.625	0.751	0.931	0.187	0.945	0.404	0.105	0.557	0.606	0.591	0.667
SH-rε	<i>r</i>	0.290	0.087	-0.061	0.257	0.250	0.219	0.265	0.189	-0.156	0.040	-0.012	0.072	-0.325	0.065	0.147
	<i>P</i>	0.202	0.699	0.793	0.260	0.262	0.328	0.245	0.413	0.500	0.861	0.960	0.749	0.151	0.792	0.513
RT-lε	<i>r</i>	0.017	-0.135	0.237	0.248	0.187	0.165	-0.046	0.160	0.451	-0.456	-0.490	0.105	0.038	-0.154	0.168
	<i>P</i>	0.939	0.530	0.276	0.253	0.382	0.441	0.839	0.467	0.031*	0.029*	0.018*	0.626	0.865	0.482	0.432
SDT-lε	<i>r</i>	0.108	-0.038	0.129	0.162	0.221	0.225	-0.087	0.150	0.472	-0.514	-0.485	-0.027	-0.008	-0.222	-0.020
	<i>P</i>	0.642	0.866	0.576	0.482	0.323	0.314	0.707	0.506	0.027*	0.014*	0.022*	0.905	0.970	0.333	0.930
SH-lε	<i>r</i>	0.199	-0.095	-0.024	0.150	0.119	0.270	0.155	-0.046	0.081	0.068	-0.345	0.009	-0.161	-0.067	0.362
	<i>P</i>	0.351	0.652	0.912	0.483	0.572	0.193	0.480	0.830	0.706	0.754	0.098	0.965	0.453	0.754	0.076
Q <sub>P-Ao</sub>	<i>r</i>	0.327	0.230	-0.089	-0.147	-0.171	-0.232	-0.292	0.724	0.205	-0.133	-0.201	-0.421	0.005	-0.127	0.060
	<i>P</i>	0.111	0.268	0.674	0.482	0.414	0.265	0.157	0.000*	0.325	0.525	0.335	0.036*	0.983	0.563	0.819

AAT: aortic outflow acceleration time, AGp: aortic outflow peak velocity pressure gradient, AVp: aortic outflow peak velocity,  $EF_M$ : ejection fraction derived from m-mode, EPSS: E point to septal separation, ESVI: end systolic volume index, FAC: fractional area change, FS: fractional shortening, IVS%: percentage thickening of the interventricular septum, LVFW%: percentage thickening of the left ventricular free wall, LVMI: left ventricular mass index, PEP:ET: pre-ejection time period and ejection time ratio, PVp: pulmonary outflow peak velocity,  $Q_{P-A0}$ : difference between pulmonary pre-ejection time, SV: stroke volume, RT-cε: range of time to peak circumferential strain, RT-lε: range of time to peak longitudinal strain, RT-rε: range of time to peak radial strain, SDT-cε: standard deviation of time to peak circumferential strain, SDT-lε: standard deviation of time to peak longitudinal strain, SDT-rε: standard deviation of time to peak radial strain, SH-cε: segmental heterogeneity in circumferential strain, SH-lε: segmental heterogeneity in longitudinal strain, SH-rε: segmental heterogeneity in radial strain, SV: stroke volume, TH-cε: transmural heterogeneity in circumferential strain, Vcf: velocity of circumferential fiber shortening;  $r$ =Spearman correlation coefficient,  $*P<0.05$  (two tail), correlation significant.



**Table 10.** Comparison MEVp, MAVp, M<sub>E/A</sub>, TEVp, TAVp, T<sub>E/A</sub>, Q<sub>P-Ao</sub>, IVRT, Tei index with heterogeneity (SH-ε, TH-ε) synchrony (RT-ε, SDT-ε)

	MEVp		MAVp		M <sub>E/A</sub>		TEVp		TAVp		T <sub>E/A</sub>		IVRT		Tei index	
	<i>r</i>	<i>P</i>	<i>r</i>	<i>P</i>	<i>r</i>	<i>P</i>	<i>r</i>	<i>P</i>	<i>r</i>	<i>P</i>	<i>r</i>	<i>P</i>	<i>r</i>	<i>P</i>	<i>r</i>	<i>P</i>
RT-cε	-0.087	0.699	-0.141	0.530	0.123	0.585	-0.148	0.523	-0.237	0.300	0.394	0.077	0.098	0.688	0.055	0.822
SDT-cε	-0.066	0.770	-0.176	0.432	0.189	0.400	-0.016	0.944	-0.200	0.385	0.398	0.074	0.025	0.918	-0.036	0.884
SH-cε	0.042	0.851	0.191	0.395	-0.220	0.326	0.434	0.049*	0.330	0.144	0.077	0.739	-0.340	0.155	-0.042	0.864
TH-cε	-0.187	0.406	-0.040	0.861	-0.085	0.708	-0.103	0.658	-0.335	0.138	0.342	0.129	-0.206	0.397	-0.177	0.468
RT-rε	-0.123	0.585	0.298	0.178	-0.470	0.027*	0.154	0.506	0.225	0.326	-0.211	0.359	-0.275	0.254	0.050	0.839
SDT-rε	-0.208	0.352	0.199	0.375	-0.412	0.056	0.100	0.668	0.157	0.496	-0.174	0.452	-0.282	0.242	0.031	0.901
SH-rε	-0.011	0.962	0.062	0.783	-0.075	0.740	0.124	0.594	0.020	0.931	0.010	0.964	-0.363	0.126	-0.411	0.081
RT-lε	-0.207	0.331	-0.109	0.613	-0.077	0.720	-0.307	0.145	-0.109	0.613	-0.110	0.610	0.489	0.025*	-0.047	0.841
SDT-lε	-0.378	0.083	-0.228	0.307	-0.008	0.972	-0.397	0.067	-0.276	0.214	0.045	0.842	0.461	0.041*	-0.026	0.912
SH-lε	-0.033	0.875	-0.092	0.661	-0.061	0.771	-0.215	0.302	-0.062	0.768	-0.176	0.399	0.011	0.962	-0.359	0.110
Q <sub>P-Ao</sub>	-0.212	0.309	-0.304	0.140	0.270	0.192	-0.151	0.482	-0.396	0.055	0.543	0.006*	0.313	0.137	0.157	0.464

IVRT: isovolumic relaxation time, MAVp: peak late mitral inflow velocity, M<sub>E/A</sub>: early and late mitral inflow ratio, MEVp: peak early mitral inflow velocity, Q<sub>P-Ao</sub>: difference between pulmonary pre-ejection time, RT-cε: range of time to peak circumferential strain, RT-lε: range of time to peak longitudinal strain, RT-rε: range of time to peak radial strain, SDT-cε: standard deviation of time to peak circumferential strain, SDT-lε: standard deviation of time to peak longitudinal strain, SDT-rε: standard deviation of time to peak radial strain, SH-cε: segmental heterogeneity in circumferential strain, SH-lε: segmental heterogeneity in longitudinal strain, SH-rε: segmental heterogeneity in radial strain, TAVp: peak late tricuspid inflow velocity, T<sub>E/A</sub>: early and late tricuspid inflow ratio, Tei index: myocardial performance index, TEVp: peak early tricuspid inflow velocity, TH-cε: transmural heterogeneity in circumferential strain. *r*=Spearman correlation coefficient, \**P*<0.05 (two tail), correlation significant.

**Table 11.** Relationship between indices of strain and strain rate and left ventricular synchrony and heterogeneity

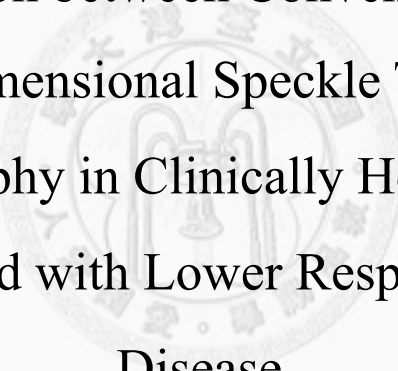
	Q <sub>P-Ao</sub>		RT-cε		SDT-cε		SH-cε		TH-cε	
	<i>r</i>	<i>P</i>	<i>r</i>	<i>P</i>	<i>r</i>	<i>P</i>	<i>r</i>	<i>P</i>	<i>r</i>	<i>P</i>
CSg	0.130	0.619	-0.150	0.504	-0.078	0.730	0.455	0.034*	-0.817	0.000*
CSRg	-0.010	0.970	-0.210	0.348	-0.128	0.571	0.392	0.071	-0.816	0.000*
CSR-Eg	0.155	0.567	-0.043	0.854	0.055	0.812	0.377	0.092	-0.747	0.000*
CSR-Ag	-0.498	0.050*	-0.378	0.091	-0.322	0.154	-0.179	0.437	-0.291	0.201
	Q <sub>P-Ao</sub>		RT-rε		SDT-rε		SH-rε			
RSg	0.065	0.804	-0.349	0.111	-0.283	0.202	0.356	0.104		
RSRg	-0.131	0.615	-0.079	0.728	-0.043	0.850	0.230	0.303		
RSR-Eg	0.135	0.617	-0.291	0.213	-0.259	0.271	0.078	0.743		
RSR-Ag	-0.401	0.124	0.223	0.345	0.229	0.332	0.215	0.363		
	Q <sub>P-Ao</sub>		RT-lε		SDT-lε		SH-lε			
LSg	0.118	0.642	0.010	0.961	-0.138	0.539	0.481	0.015*		
LSRg	0.040	0.874	0.059	0.784	-0.081	0.721	0.389	0.054		
LSR-Eg	0.137	0.672	0.006	0.982	-0.040	0.893	0.291	0.292		
LSR-Ag	-0.132	0.699	0.335	0.242	0.401	0.174	0.055	0.852		

CS: global peak circumferential strain, CSR<sub>Ag</sub>: global peak circumferential late diastolic strain rate, CSR<sub>Eg</sub>: global peak circumferential early diastolic strain rate, CSRg: global peak circumferential systolic strain rate, LS: longitudinal strain, LSR<sub>Ag</sub>: global peak longitudinal late diastolic strain rate, LSR<sub>Eg</sub>: global peak longitudinal early diastolic strain rate, LSRg: global peak longitudinal systolic strain rate, Q<sub>P-Ao</sub>: difference between pulmonary pre-ejection time and aortic pre-ejection time, RS: radial strain, RSR<sub>Ag</sub>: global peak radial late diastolic strain rate, RSR<sub>Eg</sub>: global peak radial early diastolic strain rate, RSRg: global peak radial systolic strain rate, RT-cε: range of time to peak circumferential strain, RT-lε: range of time to peak longitudinal strain, RT-rε: range of time to peak radial strain, SDT-cε: standard deviation of time to peak circumferential strain, SDT-lε: standard deviation of time to peak longitudinal strain, SDT-rε: standard deviation of time to peak radial strain, SH-cε: segmental heterogeneity in circumferential strain, SH-lε: segmental heterogeneity in longitudinal strain, SH-rε: segmental heterogeneity in radial strain, TH-cε: transmural heterogeneity in circumferential strain.

*r*=Spearman correlation coefficient, \**P*<0.05 (two tail), significant correlation.

Chapter III

Comparison between Conventional and  
Two-Dimensional Speckle Tracking  
Echocardiography in Clinically Healthy Cats and  
Cats Affected with Lower Respiratory Tract  
Disease



### Key to abbreviations

2D-STE	Two-dimensional speckle tracking echocardiography
AAT	Aortic outflow acceleration time
AGp	Aortic outflow peak velocity pressure gradient
AVp	Aortic outflow peak velocity
BW	Body weight
CS	Peak circumferential strain
CSg	Global peak circumferential strain
CSR	Peak circumferential systolic strain rate
CSR <sub>A</sub>	Peak circumferential late diastolic strain rate
CSR <sub>Ag</sub>	Global peak circumferential late diastolic strain rate
CSR <sub>E</sub>	Peak circumferential early diastolic strain rate
CSR <sub>Eg</sub>	Global peak circumferential early diastolic strain rate
CSRg	Global peak circumferential systolic strain rate
EF <sub>M</sub>	Ejection fraction derived from m-mode
EF <sub>ste</sub>	Ejection fraction derived from speckle tracking echocardiography
EPSS	E point to septal separation
ESVI	End systolic volume index
FAC	Fractional area change
FS	Fractional shortening
HR	Heart rate
IVRT	Isovolumic relaxation time
IVS%	Percentage thickening of the interventricular septum
IVSd	Interventricular septal thickness in end diastole
LA/Ao	The ratio of left atrium and aortic diameter
LS	Peak longitudinal strain
LSg	Global peak longitudinal strain
LSR	Peak longitudinal systolic strain rate
LSR <sub>A</sub>	Peak longitudinal late diastolic strain rate
LSR <sub>Ag</sub>	Global peak longitudinal late diastolic strain rate
LSR <sub>E</sub>	Peak longitudinal early diastolic strain rate
LSR <sub>Eg</sub>	Global peak longitudinal early diastolic strain rate
LSRg	Global peak longitudinal systolic strain rate
LVDd	Left ventricular dimension in end-diastole
LVDs	Left ventricular dimension in end-systole
LVPW%	Percentage thickening of the left ventricular free wall
LVPWd	Left ventricular free wall thickness in end-diastole



LVFWs	Left ventricular free wall thickness in end-systole
LVMI	Left ventricular mass index
MAvp	Peak late mitral inflow velocity
$M_{E/A}$	Early and late mitral inflow ratio
MEVp	Peak early mitral inflow velocity
PEP:ET	Pre-ejection time period and ejection time ratio
PVp	Pulmonary outflow peak velocity
$Q_{P-A_0}$	Difference between pulmonary pre-ejection time and aortic pre-ejection time
RS	Peak radial strain
RSg	Global peak radial strain
RSR	Peak radial systolic strain rate
$RSR_A$	Peak radial late diastolic strain rate
$RSR_{Ag}$	Global peak radial late diastolic strain rate
$RSR_E$	Peak radial early diastolic strain rate
$RSR_{Eg}$	Global peak radial early diastolic strain rate
RSRg	Global peak radial systolic strain rate
RT-c $\epsilon$	Range of the 6 segment time to peak circumferential strain
RT-l $\epsilon$	Range of the 6 segment time to peak longitudinal strain
RT-r $\epsilon$	Range of the 6 segment time to peak radial strain
RT- $\epsilon$	Range of the 6 segment time to peak strain
SDT-c $\epsilon$	Standard deviation of the 6 segment time to peak circumferential strain
SDT-l $\epsilon$	Standard deviation of the 6 segment time to peak longitudinal strain
SDT-r $\epsilon$	Standard deviation of the 6 segment time to peak radial strain
SDT- $\epsilon$	Standard deviation of the 6 segment time to peak strain
Sg	Global peak strain
SH-c $\epsilon$	Circumferential segmental heterogeneity
SH-l $\epsilon$	Longitudinal segmental heterogeneity
SH-r $\epsilon$	Radial segmental heterogeneity
SH- $\epsilon$	Segmental heterogeneity
SR	Peak systolic strain rate
$SR_A$	Peak late diastolic strain rate
$SR_{Ag}$	Global peak late diastolic strain rate
$SR_E$	Peak early diastolic strain rate
$SR_{Eg}$	Global peak early diastolic strain rate
SRg	Global peak strain rate
SV	Stroke volume

TAVp	Peak late tricuspid inflow velocity
T <sub>E/A</sub>	Early and late tricuspid inflow ratio
Tei index	Myocardial performance index
TEVp	Peak early tricuspid inflow velocity
TH-ε	Transmural heterogeneity
Vcf	Velocity of circumferential fiber shortening
ε	Langarian strain



## **Comparison between Conventional and Two-Dimensional Speckle Tracking Echocardiography in Clinically Healthy Cats and Cats Affected with Lower Respiratory Tract Disease**

Yueh-Lun Hsu, Hui-Pi Huang

Department of Veterinary Medicine, National Taiwan University, Taipei, Taiwan

### **Abstract**

Feline lower respiratory tract disease (LRTD), also known as asthma, is a syndrome characterized by acute bronchoconstriction, the clinical sign of which is similar to cardiac failure. The aim of this study was to analyze left ventricular deformation change by application of 2D-STE in cats with LRTD.

Fifty-six cats were included in this study. These cats were further categorized into clinically healthy control (n=34) and LRTD (n=22). Physical examinations, blood pressure measurement, routine blood examinations, chest radiographs, conventional echocardiography and 2D-STE were carried out in all cats in both groups.

Indices of conventional echocardiography were not different between two groups, but impaired systolic and diastolic function was detected in LRTD based on using circumferential/longitudinal strain of 2D-STE. Decreased transmural heterogeneity and ejection fraction/fractional area change those were derived from 2D-STE were also found. No difference in synchrony and heterogeneity were detected between two groups.

The deformation changes mainly affected the segments of the left ventricle free wall. In the cats with LRTD, no change in stroke volume and end diastolic dimension were detected, no pulmonary to tricuspid regurgitation was identified either. These findings suggested that even in a very mild degree of lower respiratory tract disease the function of the left ventricle could be affected.

Key words: cat, left ventricle, lower respiratory tract disease, two-dimensional speckle tracking echocardiography

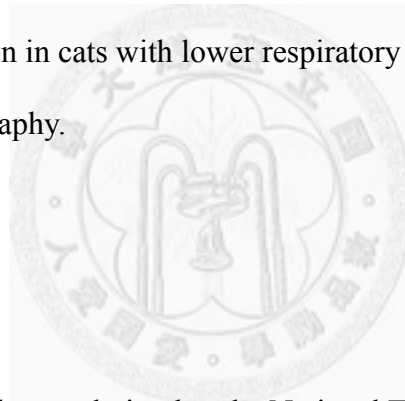
---

Part of the study was presented as an abstract in the 21<sup>th</sup> European College of Veterinary Internal Medicine Congress, Seville, Spain. Sep. 8-10, 2011.

## **Introduction**

The impact of respiratory diseases on cardiac function has been intensively discussed in past fifty years in human patients. Changes in the volume or pressure of right ventricular may affect the condition of systole and diastole in left ventricle via pericardium and interventricular septum (ventricular interdependence) [1-5].

Feline lower respiratory tract disease (LRTD), also known as asthma, is a syndrome characterized by acute bronchoconstriction that can lead to cough and respiratory distress [6]. These clinical signs are also consistent with left sided heart failure in cats [7]. Study regarding cardiac function in association with respiratory diseases in cats is very limited. The aims of this study were to assess cardiac function and myocardial deformation in cats with lower respiratory tract using different modalities of echocardiography.



## **Material and Method**

### **Animals**

Fifty-six client-owned cats admitted to the National Taiwan University Veterinary Hospital during 2010-2012 were included for this perspective study. These cats were further categorized into groups of clinically healthy control and LRTD. All cats underwent a complete physical examination, blood pressure measurements, routine blood work (complete blood counts and biochemical profiles) examinations, chest radiography, conventional echocardiography, and two-dimensional speckle-tracking echocardiography (2D-STE).

### ***Clinically healthy cats (control)***

Among these 56 cats, 34 that were clinically healthy cats for annual wellness recheck and without history of respiratory signs were deemed as healthy controls in

this study. The mean age was  $3.1 \pm 2.2$  years (range 6 months to 8 years old), with a mean body weight of  $4.3 \pm 1.3$  kg; 18 were males, and 16 were females. Breeds represented in this group were 19 Domestic Short-hairs, 6 American Short-hairs, 7 Persians, 1 Bengal cat and 1 British Blue.

#### ***Cats with lower respiratory tract disease (LRTD)***

The remaining 22 cats that were presented with intermittent to continuous respiratory signs (cough, respiratory distress and open mouth breathing) were categorized into LRTD group. The inclusion criteria of LRTD in this group were based on clinical signs, chest radiographs [8, 9], and results of provocative barometric whole-body plethysmography test. The mean age of this group was  $5.0 \pm 3.4$  (range of 5 month to 12 years). A mean body weight was  $4.5 \pm 0.9$  kg, 12 were males, and 10 were females. The represented breeds were 12 Domestic short-hairs, 3 each of Persians and Himalayas, 2 American short-hairs, and 1 each of English short-haired and Siamese crossed bred

#### **Clinical evaluation**

##### ***Conventional echocardiography***

Ultrasound examinations were performed without sedation with gentle restrain in lateral recumbency [10].

Indices of left ventricle was including left ventricular diastolic dimension (LVDd), left ventricular systolic dimension (LVDs), the ratio of Left atrium and aortic diameter (LA/Ao), interventricular septal thickness in diastole (IVSd), left ventricular free wall thickness in diastole (LVFWd), and left ventricular mass index (LVMI) were obtained from the standard views [11, 12].

Parameters of left ventricular systolic function were derived from M-mode, including end-posterior E point to septal separation (EPSS), percentage thickening of

the interventricular septum (IVS%), percentage thickening of the left ventricular free wall (LVFW%), fractional shortening (FS), ejection fraction by M-mode ( $EF_M$ ); parameters were derived from pulse-wave Doppler including velocity of circumferential fiber shortening (Vcf), the ratio of pre-ejection period and ejection time (PEP:ET), Aortic outflow acceleration time (AAT), including aortic outflow peak velocity (AVp), aortic outflow peak velocity pressure gradient (AGp), pulmonary outflow peak velocity (PVp), stroke volume (SV), and derived from B mode, including end systolic volume index (ESVI) were obtained from the standard views [12-21].

Parameters of left ventricular diastolic function were including mitral early and late diastolic inflow velocity (MEVp, MAVp), and tricuspid early and late diastolic inflow velocity (TEVp, TAVp), the ratio between MEVp and MAVp ( $M_{E/A}$ ), the ratio between TEVp and TAVp ( $T_{E/A}$ ), isovolumic relaxation time (IVRT), and myocardial performance index (Tei index) were obtained from the standard views [14, 22, 23].

Interventricular synchrony, the difference between pulmonary pre-ejection time and aortic pre-ejection time ( $Q_{P-Ao}$ ) was obtained from standard views [24].

### ***Two-dimensional speckle tracking echocardiography***

#### ***Measurement regional strain and strain rate***

Indices of left ventricular longitudinal and circumferential/radial/longitudinal strain and strain rates were obtained using right parasternal apical 4-chamber and short axis views, respectively. All images were acquired in cine loops of 3 cardiac cycles recorded at frame rate of 54-111 frames per seconds, saved in digital format, and analyzed by off-line software (XStrain<sup>TM</sup> software for MyLab<sup>TM</sup>50 X Vision).

In quantification of strain and strain, 6 segments (cranio-septum, cranial, lateral, caudal, ventral, and septal) of endocardium and another 6 segments of epicardium for

epicardial circumferential strain were semi-automatically selected by Aided Heart Segmentation (AHS) for analysis; 6 segments (craniao-septum, cranial, lateral, caudal, ventral, and septal) across endocardium to epicardium were semi-automatically selected by AHS for radial strain analysis. In left ventricular longitudinal strain and strain rate, 6 segments (basal-septal, mid-septal, apical-septal, apical-lateral, mid-lateral, basal-lateral) of endocardium were semi-automatically automatically selected by the AHS tool for analysis. Left ventricular ejection volume ( $EF_{ste}$ ) and fraction area change (FAC) were also calculated by modified Simpson's rule.

The STE indices included in this study were circumferential/radial/longitudinal systolic peak strain (CS/RS/LS), circumferential/radial/longitudinal systolic peak strain rate (CRS/RSR/LSR), circumferential/radial/longitudinal peak early diastolic strain rate ( $CSR_E/RSR_E/LSR_E$ ) and circumferential/radial/longitudinal peak late diastolic strain rate ( $CSR_A/RSR_A/LSR_A$ ). The STE off-line analysis was performed by 1 examiner (YLH)

The images without adequate visualization of one or more segments of the endocardium were excluded from this study.

### ***Measurement of synchrony and heterogeneity***

Interventricular synchrony, defined as time difference between mean pulmonary and aortic pre-ejection periods ( $Q_{P-Ao}$ ), was calculated based on conventional pulse wave-Doppler. Intraventricular synchrony, defined as the standard deviation of the six segments time to reach peak strain (SDT- $\epsilon$ ) at longitudinal (SDT-l $\epsilon$ ), circumferential (SDT-c $\epsilon$ ) and radial (SDT-r $\epsilon$ ) directions, and the range of the six segments time to peak strain (RT- $\epsilon$ ) at longitudinal (RT-l $\epsilon$ ), circumferential (RT-c $\epsilon$ ) and radial (RT-r $\epsilon$ ) directions were also calculated. Segmental heterogeneity (SH- $\epsilon$ ), defined as the range of the peak strain of the six segments, and transmural heterogeneity (TH- $\epsilon$ ), defined as

the difference strain between endocardium and epicardium were also calculated

### **Statistical analysis**

Continuous data are presented as mean  $\pm$  SD. Normality was assessed by using Kolmogorov-Smirnov test. Group data of conventional echocardiography (LVMI, IVSd, LFFWd, LVDd, LVDs, LA/Ao; EPSS, IVS%, LVFW%, FS, EF<sub>M</sub>; PEP:ET, AAT, AVp, AGp, PVp SV, mitral inflow, tricuspid inflow, IVRT and Tei index; Vcf) and STE (strain, SR, FAC, EF<sub>ste</sub>) were compared using 2-tailed independent Student t-test. In the event of cohorts of variables without a normal distribution, comparisons were done with Mann-Whitney U test.  $P < 0.05$  were considered to be statistically significant.

### **Results**

The demographic information of control and LRTD is listed at Table 1. Gender ( $P=0.906$ ) and age ( $P=0.054$ ) were not different between these two groups, heart rate was significantly higher in LRTD ( $P < 0.005$ , Table 4-6).

### **Indices of conventional echocardiography**

Differences of left ventricular indices, including LVMI, IVSd, LVFWd, LVDd, LVDs and LA/Ao were all not significant (Table 2). Indices derived from M-mode (EPSS, IVS%, LVFW%, FS and EF<sub>M</sub>), and from pulse-wave Doppler (PEP: ET, AAT, AVp, AGp, PVp SV, mitral inflow, tricuspid inflow, IVRT and Tei index) and Vcf were not different between these 2 groups (Table 3).

### **Indices derived from myocardial strain**

Global CS, CSR<sub>g</sub>, and CSR<sub>Eg</sub> were significantly decreased in LRTD group (Table 4). Global radial strain and strain rate were not different between control and



LRTD (Table 5). Global LS and LSRg were significantly decreased in LRTD group (Table 6).

### **EF<sub>ste</sub> and FAC**

The EF<sub>ste</sub> and FAC derived from speckle tracking echocardiography were significantly decreased in LRTD (Table 7).

### **Synchrony and heterogeneity**

Indices of ventricular synchrony were not different between control and LRTD (Table 8). Segmental heterogeneity was not different between control and LRTD (Table 8). Circumferential transmural heterogeneity was significantly decreased in LRTD ( $P=0.034$ , Table 8).

### **Discussion**

Left sided heart failure and LRTD share similar clinical signs, cough and respiratory distress. These two conditions cannot be discriminated by the heart rate or absence of cardiac murmurs. Absence of murmur is prevalent in cats with clinical signs of heart failure [25-28]. In this study, indices derived from conventional echocardiography in control and LRTD were not different. This finding suggests that echocardiography may distinguish LRTD from left sided heart failure if results of physical examination or chest radiographs are not conclusive. Indices of echocardiography are normal in coughing cats are highly unlikely to be affected with cardiac disease.

Although no difference of indices derived from conventional echocardiography was found between control and LRTD, significantly decreased left ventricular strain in circumferential and longitudinal systole and significantly decreased circumferential

early diastole were found in this study. Decreased transmural heterogeneity was also found in cats with LRTD. Changes in the volume or pressure of right ventricular may influence the condition of systole and diastole in left ventricle via the pericardium and interventricular septum. In this study, decreasing systolic function in terms of reduces  $EF_{ste}$  / FAC, also reflected the decreasing transmural heterogeneity in cats with LRTD[29]. The decreasing pattern of our finding was different comparing with the human patients suffering from pulmonary disorders/hypertension [30-32]. Ventricular interdependence has been exhibited in human patients with pulmonary hypertension [33]. Interventricular septum plays an important role in ventricular interdependence. Impact of pressure gradient between right and left ventricles, pulmonary hypertension resulted from chronic hypoxia and volume expansion of right ventricle may indirectly affect compliance of interventricular septum and left ventricular deformation [2, 3, 5, 33-35]. Left ventricular dyssynchrony may develop eventually [36]. However, in this study no ventricular dyssynchrony and segmental heterogeneity was detected in LRTD. The affected segments were mainly on the free wall of left ventricle. The mechanism of the discrepancies was not clear. Nevertheless, no pulmonary or tricuspid regurgitation was detected in our cases. In addition, the end diastole dimension and stroke volume were not different from the control. This suggested that pulmonary hypertension had not yet developed in these cases. Impact of pressure or volume right ventricle on the interventricular septum and left ventricle might be subtle at this stage. Only decreased myocardial strain and  $EF_{ste}$ /FAC derived from strain were detected. These findings supported that the LS of left ventricle has decreased before decreasing systolic function right ventricle has developed in asthma patients [32].

Longitudinal study is needed to clarify the impact of decreasing strain and strain

rate in LRTD group and further provide prognostic and diagnostic value in clinical application.

## Conclusion

Impaired systolic and diastolic function of left ventricle was developed as mild as the secondary pulmonary hypertension and ventricular interdependence could not be detected by the conventional echocardiography.

## Reference

1. Jessup M, Sutton MSJ, Weber KT, Janicki JS: **The effect of chronic pulmonary hypertension on left ventricular size, function, and interventricular septal motion.** *Am Heart J* 1987, **113**:1114-1122.
2. Leichsenring-Silva F, Tavares AMV, Mosele F, Berger B, Llesuy S, Belló-Klein A: **Association of the time course of pulmonary arterial hypertension with changes in oxidative stress in the left ventricle.** *Clin Exp Pharmacol Physiol* 2011, **38**:804-810.
3. Stool EW, Mullins CB, Leshin SJ, Mitchell JH: **Dimensional changes of the left ventricle during acute pulmonary arterial hypertension in dogs.** *Am J Cardiol* 1974, **33**:868-875.
4. Menzel T, Wagner S, Kramm T, Mohr-Kahaly S, Mayer E, Braeuninger S, Meyer J: **Pathophysiology of impaired right and left ventricular function in chronic embolic pulmonary hypertension : changes after pulmonary thromboendarterectomy.** *Chest* 2000, **118**:897-903.
5. Boussuges A, Pinet C, Molenat F, Burnet h, Ambrosi P, Badier M, Sainty JM, Orehek J: **Left atrial and ventricular filling in chronic obstructive pulmonary disease.** *Am J Respir Crit Care Med* 2000, **162**:670-675.
6. Hirt RA, Galler A, Shibly S, Bilek A: **Airway hyperresponsiveness to adenosine 5'-monophosphate in feline chronic inflammatory lower airway disease.** *Vet J* 2011, **187**:54-59.
7. Atkins C, Gallo A, Kurzman I, Cowen P: **Risk factors, clinical signs, and survival in cats with a clinical diagnosis of idiopathic hypertrophic cardiomyopathy: 74 cases (1985-1989).** *J Am Vet Med Assoc* 1992, **201**:613-618.
8. Gadbois J, d'Anjou MA, Dunn M, Alexander K, Beauregard G, D'Astous J, De

- Carufel M, Breton L, Beauchamp G: **Radiographic abnormalities in cats with feline bronchial disease and intra-and interobserver variability in radiographic interpretation: 40 cases (1999–2006)**. *J Am Vet Med Assoc* 2009, **234**:367-375.
9. Corcoran B, Foster D, Fuentes VL: **Feline asthma syndrome: a retrospective study of the clinical presentation in 29 cats**. *J Small Anim Pract* 1995, **36**:481-488.
  10. Thomas WP, Gaber CE, Jacobs GJ, Kaplan PM, Lombard CW, Moise N, Moses BL: **Recommendations for Standards in Transthoracic Two-Dimensional Echocardiography in the Dog and Cat**. *J Vet Intern Med* 1993, **7**:247-252.
  11. Troy BL, Pombo J, Rackley CE: **Measurement of left ventricular wall thickness and mass by echocardiography**. *Circulation* 1972, **45**:602-611.
  12. Lang RM, Bierig M, Devereux RB, Flachskampf FA, Foster E, Pellikka PA, Picard MH, Roman MJ, Seward J, Shanewise JS: **Recommendations for chamber quantification: a report from the American Society of Echocardiography's Guidelines and Standards Committee and the Chamber Quantification Writing Group, developed in conjunction with the European Association of Echocardiography, a branch of the European Society of Cardiology**. *J Am Soc Echocardiogr* 2005, **18**:1440-1463.
  13. Massie BM, Schiller NB, Ratshin RA, Parmley WW: **Mitral-septal separation: new echocardiographic index of left ventricular function**. *Am J Cardiol* 1977, **39**:1008-1016.
  14. Schwarz T, Johnson V: *BSAVA manual of canine and feline thoracic imaging*: Gloucester: British Small Animal Veterinary Association; 2008.
  15. Folland E, Parisi A, Moynihan P, Jones DR, Feldman C, Tow D: **Assessment of left ventricular ejection fraction and volumes by real-time, two-dimensional echocardiography. A comparison of cineangiographic and radionuclide techniques**. *Circulation* 1979, **60**:760-766.
  16. Sigurdardóttir L, Helgason H: **Echocardiographic evaluation of systolic and diastolic function in postoperative coarctation patients**. *Pediatr Cardiol* 1997, **18**:96-100.
  17. Burwash IG, Otto CM, Pearlman AS: **Use of Doppler-derived left ventricular time intervals for noninvasive assessment of systolic function**. *Am J Cardiol* 1993, **72**:1331-1333.
  18. Ben Zekry S, Saad RM, Ozkan M, Al Shahid MS, Pepi M, Muratori M, Xu J, Little SH, Zoghbi WA: **Flow Acceleration Time and Ratio of Acceleration Time to Ejection Time for Prosthetic Aortic Valve Function**. *JACC*

- Cardiovasc Imaging* 2011, **4**:1161-1170.
19. Singer M, Allen MJ, Webb AR, Bennett ED: **Effects of alterations in left ventricular filling, contractility, and systemic vascular resistance on the ascending aortic blood velocity waveform of normal subjects.** *Crit Care Med* 1991, **19**:1138-1145.
  20. Lewis J, Kuo L, Nelson J, Limacher M, Quinones M: **Pulsed Doppler echocardiographic determination of stroke volume and cardiac output: clinical validation of two new methods using the apical window.** *Circulation* 1984, **70**:425-431.
  21. Borow KM, Green LH, Mann T, Sloss LJ, Braunwald E, Collins Jr JJ, Cohn L, Grossman W: **End-systolic volume as a predictor of postoperative left ventricular performance in volume overload from valvular regurgitation.** *Am J Med* 1980, **68**:655-663.
  22. Santilli RA, Bussadori C: **Doppler echocardiographic study of left ventricular diastole in non-anaesthetized healthy cats.** *Vet J.* 1998, **156**:203-215.
  23. Tei C, Nishimura RA, Seward JB, Tajik AJ: **Noninvasive Doppler-derived myocardial performance index: correlation with simultaneous measurements of cardiac catheterization measurements.** *J Am Soc Echocardiogr* 1997, **10**:169-178.
  24. López-Alvarez J, Fonfara S, Pedro B, Stephenson H, Cripps PJ, Dukes-McEwan J: **Assessment of mechanical ventricular synchrony in Doberman Pinscher with dilated cardiomyopathy.** *J Vet Cardiol* 2011, **13**:183-195.
  25. Nakamura RK, Rishniw M, King MK, Sammarco CD: **Prevalence of echocardiographic evidence of cardiac disease in apparently healthy cats with murmurs.** *J Feline Med Surg* 2011, **13**:266-271.
  26. Wagner T, Fuentes VL, Payne JR, McDermott N, Brodbelt D: **Comparison of auscultatory and echocardiographic findings in healthy adult cats.** *J Vet Cardiol* 2010, **12**:171-182.
  27. Côté E, Manning AM, Emerson D, Laste NJ, Malakoff RL, Harpster NK: **Assessment of the prevalence of heart murmurs in overtly healthy cats.** *J Am Vet Med Assoc* 2004, **225**:384-388.
  28. Smith S, Dukes-McEwan J: **Clinical signs and left atrial size in cats with cardiovascular disease in general practice.** *J Small Anim Pract* 2011, **53**:27-33.
  29. Moore CC, Lugo-Olivieri CH, McVeigh ER, Zerhouni EA: **Three-dimensional Systolic Strain Patterns in the Normal Human Left**

- Ventricle: Characterization with Tagged MR Imaging**<sup>1</sup>. *Radiology* 2000, **214**:453-466.
30. Olson N, Brown JP, Kahn AM, Auger WR, Madani MM, Waltman TJ, Blanchard DG: **Left ventricular strain and strain rate by 2D speckle tracking in chronic thromboembolic pulmonary hypertension before and after pulmonary thromboendarterectomy**. *Cardiovasc Ultrasound* 2010, **8**:43.
  31. Ramani GV, Bazaz R, Edelman K, Lopez-Candales A: **Pulmonary hypertension affects left ventricular basal twist: a novel use for speckle-tracking imaging**. *Echocardiography* 2009, **26**:44-51.
  32. Rajdev S, Nanda NC, Patel V, Singh A, Mehmood F, Vengala S, Fang L, Dasan V, Benza RL, Bourge RC: **Tissue Doppler assessment of longitudinal right and left ventricular strain and strain rate in pulmonary artery hypertension**. *Echocardiography* 2006, **23**:872-879.
  33. Puwanant S, Park M, Popović ZB, Tang WHW, Farha S, George D, Sharp J, Puntawangkoon J, Loyd JE, Erzurum SC: **Ventricular geometry, strain, and rotational mechanics in pulmonary hypertension**. *Circulation* 2010, **121**:259-266.
  34. Gomez A, Mink S: **Increased left ventricular stiffness impairs filling in dogs with pulmonary emphysema in respiratory failure**. *J Clin Invest* 1986, **78**:228-240.
  35. Gomez A, Unruh H, Mink SN: **Altered left ventricular chamber stiffness and isovolumic relaxation in dogs with chronic pulmonary hypertension caused by emphysema**. *Circulation* 1993, **87**:247-260.
  36. Dohi K, Onishi K, Gorcsan III J, López-Candales A, Takamura T, Ota S, Yamada N, Ito M: **Role of radial strain and displacement imaging to quantify wall motion dyssynchrony in patients with left ventricular mechanical dyssynchrony and chronic right ventricular pressure overload**. *Am J Cardiol* 2008, **101**:1206-1212.

**Table 1.** Comparison of demographics between clinically healthy cats (control) and cats with lower respiratory tract disease (LRTD)

	Control (n=34)	LRTD (n=22)	<i>P</i>
Age (years)	3.11 ± 2.17	4.96 ± 3.42	0.054
Body weight (kg)	4.32 ± 1.32	4.46 ± 0.94	0.661
Sex	Male : female =18 : 16	Male : female =12 : 10	0.906
Heart rate (beats/min)	171.97 ± 27.23	182.05 ± 29.23	0.151
Systemic blood pressure (mmHg)	119.47 ± 15.15	115.24 ± 29.79	0.985

*P*<0.05 (two tail), statistically significant.



**Table 2.** Comparison of left ventricular indices between clinically healthy cats (control) and acts with lower respiratory tract disease (LRTD)

	Control (n=34)	LRTD (n=22)	<i>P</i>
LVMI (g/m <sup>2</sup> )	28.53 ± 7.31	27.19 ± 6.08	0.484
IVSd (mm)	4.08 ± 0.61	3.87 ± 0.54	0.236
LVFWd (mm)	4.17 ± 0.65	4.14 ± 0.62	0.889
LVDd (mm)	14.98 ± 1.63	15.21 ± 1.73	0.624
LVDs (mm)	6.81 ± 1.58	6.89 ± 1.47	0.854
LA/Ao	1.35 ± 0.16	1.36 ± 0.17	0.811

IVSd: interventricular septal thickness in end diastole, LA/Ao: the ratio of left atrium and aortic diameter, LVDd: left ventricular dimension in end-diastole, LVDs: left ventricular dimension in end-systole, LVFWd: left ventricular free wall thickness in end-diastole, LVMI: left ventricular mass index.

*P*<0.05 (two tail), statistically significant.





**Table 3.** Comparison of indices derived from conventional echocardiography between clinically healthy cats (control) and acts with lower respiratory tract disease (LRTD)

	Control (n=34)	LRTD (n=22)	<i>P</i>
EPSS (mm)	0.43 ± 0.25	0.52 ± 0.29	0.451
IVS % (%)	69.66 ± 17.84	72.61 ± 1.35	0.583
LVFW% (%)	63.19 ± 15.24	63.12 ± 18.28	0.989
FS (%)	54.74 ± 8.01	54.30 ± 6.75	0.832
EF <sub>M</sub> (%)	87.24 ± 6.53	87.52 ± 5.63	0.866
Vcf (circumferences/s)	0.38 ± 0.07	0.39 ± 0.08	0.693
PEP:ET	0.29 ± 0.08	0.29 ± 0.07	0.869
AAT (ms)	25.53 ± 7.74	26.93 ± 12.10	0.870
AVp (m/s)	0.95 ± 0.20	0.93 ± 0.22	0.762
AGp (mmHg)	1.12 ± 0.43	1.13 ± 0.51	0.820
PVp (m/s)	0.90 ± 0.18	0.93 ± 0.22	0.565
SV (ml)	354.1 ± 97.93	364.88 ± 7.86	0.785
ESVI (ml/m <sup>2</sup> )	5.11 ± 1.96	6.12 ± 2.77	0.145
MEVp (m/s)	0.82 ± 0.14	0.82 ± 0.15	0.863
MAVp (m/s)	0.68 ± 0.16	0.74 ± 0.23	0.282
M <sub>E/A</sub>	1.25 ± 0.27	1.19 ± 0.31	0.474
TEVp (m/s)	0.65 ± 0.15	0.59 ± 0.13	0.102
TAVp (m/s)	0.52 ± 0.14	0.50 ± 0.14	0.424
T <sub>E/A</sub>	1.29 ± 0.27	1.21 ± 0.27	0.297
Q <sub>P-A0</sub> (ms)	-3.90 ± 13.22	-5.46 ± 13.06	0.708
IVRT (ms)	44.17 ± 7.42	42.54 ± 8.35	0.480
Tei index	0.51 ± 0.09	0.86 ± 1.44	0.586

AAT: aortic outflow acceleration time, AGp: aortic outflow peak velocity pressure gradient, AVp: aortic outflow peak velocity, EF<sub>M</sub>: ejection fraction derived from m-mode, EPSS: E point to septal separation, ESVI: end systolic volume index, FS: fractional shortening, IVRT: isovolumic relaxation time, IVS %: percentage thickening of the interventricular septum, LVFW%: percentage thickening of the left ventricular free wall, MAVp: peak late mitral inflow velocity, M<sub>E/A</sub>: early and late mitral inflow ratio, MEVp: peak early mitral inflow velocity, PEP:ET: pre-ejection time period and ejection time ratio, PVp: pulmonary outflow peak velocity, Q<sub>P-A0</sub>: difference between pulmonary pre-ejection time and aortic pre-ejection time, SV: stroke volume, TAVp: peak late tricuspid inflow velocity, T<sub>E/A</sub>: early and late tricuspid inflow ratio, Tei index: myocardial performance index, TEVp: peak early tricuspid inflow velocity, Vcf: velocity of circumferential fiber shortening.

*P*<0.05 (two tail), statistically significant.

**Table 4.** Comparison of circumferential strain and strain rate between clinically healthy cats (control) and acts with lower respiratory tract disease (LRTD)

Circumferential	Control (n=34)	LRTD (n=22)	<i>P</i>
Heart rate (bpm)	161.27 ± 23.38	187.62 ± 28.80	0.002
CS <sub>1</sub> (%)	-21.87 ± 6.69	-14.92 ± 5.72	0.001
CS <sub>2</sub> (%)	-21.83 ± 6.40	-14.86 ± 4.29	0.000
CS <sub>3</sub> (%)	-21.82 ± 5.97	-15.87 ± 6.05	0.002
CS <sub>4</sub> (%)	-21.98 ± 7.81	-17.46 ± 5.44	0.034
CS <sub>5</sub> (%)	-21.90 ± 8.52	-19.67 ± 6.91	0.466
CS <sub>6</sub> (%)	-23.03 ± 7.15	-18.94 ± 7.42	0.073
CSg (%)	-22.26 ± 5.01	-16.95 ± 4.15	0.001
CSR <sub>1</sub> (s <sup>-1</sup> )	-2.60 ± 0.78	-1.74 ± 0.53	0.00014
CSR <sub>2</sub> (s <sup>-1</sup> )	-2.73 ± 0.97	-1.87 ± 0.37	0.001
CSR <sub>3</sub> (s <sup>-1</sup> )	-2.77 ± 0.95	-2.11 ± 0.89	0.024
CSR <sub>4</sub> (s <sup>-1</sup> )	-2.75 ± 1.21	-2.22 ± 0.81	0.152
CSR <sub>5</sub> (s <sup>-1</sup> )	-2.73 ± 1.17	-2.58 ± 0.95	0.952
CSR <sub>6</sub> (s <sup>-1</sup> )	-2.61 ± 0.87	-2.28 ± 0.97	0.244
CSRg	-2.7 ± 0.72	-2.13 ± 0.51	0.005
CSR <sub>E1</sub> (s <sup>-1</sup> )	2.71 ± 1.33	1.45 ± 0.83	0.007
CSR <sub>E2</sub> (s <sup>-1</sup> )	2.33 ± 1.09	1.45 ± 0.63	0.014
CSR <sub>E3</sub> (s <sup>-1</sup> )	2.35 ± 1.00	1.60 ± 0.62	0.026
CSR <sub>E4</sub> (s <sup>-1</sup> )	2.22 ± 1.41	1.91 ± 0.75	0.503
CSR <sub>E5</sub> (s <sup>-1</sup> )	2.33 ± 1.39	1.76 ± 0.83	0.213
CSR <sub>E6</sub> (s <sup>-1</sup> )	2.53 ± 0.91	1.65 ± 0.86	0.010
CSR <sub>Eg</sub> (s <sup>-1</sup> )	2.39 ± 0.81	1.59 ± 0.70	0.003
CSR <sub>A1</sub> (s <sup>-1</sup> )	0.99 ± 0.38	1.12 ± 0.71	0.561
CSR <sub>A2</sub> (s <sup>-1</sup> )	0.99 ± 0.23	0.95 ± 0.53	0.794
CSR <sub>A3</sub> (s <sup>-1</sup> )	1.13 ± 0.51	1.66 ± 1.66	0.410
CSR <sub>A4</sub> (s <sup>-1</sup> )	1.15 ± 0.74	1.43 ± 1.35	0.517
CSR <sub>A5</sub> (s <sup>-1</sup> )	1.33 ± 0.63	1.42 ± 0.88	0.762
CSR <sub>A6</sub> (s <sup>-1</sup> )	1.21 ± 0.48	1.53 ± 0.82	0.335
CSR <sub>Ag</sub> (s <sup>-1</sup> )	1.16 ± 0.32	1.34 ± 0.95	0.470

C<sub>1</sub>: cranio-septal, C<sub>2</sub>: cranial, C<sub>3</sub>: lateral, C<sub>4</sub>: caudal, C<sub>5</sub>: ventral, C<sub>6</sub>: septal, Cg: global, CS: peak circumferential strain, CSR: peak circumferential strain rate, CSR<sub>A</sub>: peak circumferential late diastolic strain rate, CSR<sub>E</sub>: peak circumferential early diastolic strain rate.

*P*<0.05 (two tail), statistically significant.

**Table 5.** Comparison of radial strain and strain rate between clinically healthy cats (control) and acts with lower respiratory tract disease (LRTD)

Radial	Control (n=34)	LRTD (n=22)	<i>P</i>
Heart rate(bpm)	162.00 ± 22.92	188.86 ± 31.51	0.003
RS <sub>1</sub> (%)	26.32 ± 11.64	21.34 ± 17.62	0.279
RS <sub>2</sub> (%)	25.50 ± 13.58	21.17 ± 18.06	0.378
RS <sub>3</sub> (%)	27.12 ± 12.76	21.30 ± 18.07	0.228
RS <sub>4</sub> (%)	27.38 ± 10.36	19.56 ± 17.30	0.198
RS <sub>5</sub> (%)	28.68 ± 10.04	21.20 ± 19.25	0.123
RS <sub>6</sub> (%)	29.46 ± 12.71	23.19 ± 19.86	0.229
RSg (%)	26.08 ± 8.18	21.29 ± 16.51	0.241
RSR <sub>1</sub> (s <sup>-1</sup> )	2.40 ± 0.82	2.53 ± 1.08	0.961
RSR <sub>2</sub> (s <sup>-1</sup> )	2.38 ± 1.02	2.53 ± 1.04	0.680
RSR <sub>3</sub> (s <sup>-1</sup> )	2.46 ± 0.95	2.62 ± 1.10	0.608
RSR <sub>4</sub> (s <sup>-1</sup> )	2.43 ± 0.84	2.55 ± 1.10	0.686
RSR <sub>5</sub> (s <sup>-1</sup> )	2.67 ± 1.00	2.84 ± 1.30	0.615
RSR <sub>6</sub> (s <sup>-1</sup> )	2.74 ± 1.00	2.85 ± 1.37	0.781
RSR <sub>g</sub> (s <sup>-1</sup> )	2.51 ± 0.71	2.65 ± 0.98	0.591
RSR <sub>-E1</sub> (s <sup>-1</sup> )	-2.18 ± 1.59	-1.67 ± 1.01	0.358
RSR <sub>-E2</sub> (s <sup>-1</sup> )	-2.09 ± 1.20	-1.68 ± 0.91	0.376
RSR <sub>-E3</sub> (s <sup>-1</sup> )	-2.28 ± 1.06	-1.54 ± 0.94	0.107
RSR <sub>-E4</sub> (s <sup>-1</sup> )	-1.89 ± 1.01	-1.96 ± 1.48	0.888
RSR <sub>-E5</sub> (s <sup>-1</sup> )	-1.92 ± 1.26	-2.15 ± 0.90	0.632
RSR <sub>-E6</sub> (s <sup>-1</sup> )	-2.06 ± 1.56	-1.71 ± 1.14	0.492
RSR <sub>-Eg</sub> (s <sup>-1</sup> )	-1.99 ± 1.12	-1.61 ± 0.80	0.246
RSR <sub>-A1</sub> (s <sup>-1</sup> )	-1.62 ± 0.93	-2.14 ± 1.36	0.227
RSR <sub>-A2</sub> (s <sup>-1</sup> )	-1.55 ± 0.82	-1.97 ± 1.55	0.386
RSR <sub>-A3</sub> (s <sup>-1</sup> )	-1.69 ± 0.93	-2.48 ± 1.76	0.166
RSR <sub>-A4</sub> (s <sup>-1</sup> )	-1.70 ± 0.90	-1.82 ± 1.26	0.790
RSR <sub>-A5</sub> (s <sup>-1</sup> )	-1.80 ± 0.88	-1.19 ± 0.52	0.079
RSR <sub>-A6</sub> (s <sup>-1</sup> )	-1.92 ± 1.10	-1.69 ± 1.76	0.674
RSR <sub>-Ag</sub> (s <sup>-1</sup> )	-1.82 ± 0.85	-1.74 ± 1.62	0.852

R<sub>1</sub>: cranio-septal, R<sub>2</sub>: cranial, R<sub>3</sub>: lateral, R<sub>4</sub>: caudal, R<sub>5</sub>: ventral, R<sub>6</sub>: septal, Rg: global, RS: peak radial strain, RSR: peak radial strain rate, RSR<sub>-A</sub>: peak radial late diastolic strain rate, RSR<sub>-E</sub>: peak radial early diastolic strain rate.

*P*<0.05 (two tail), statistically significant.

**Table 6.** Comparison of longitudinal strain and strain rate between clinically healthy cats (control) and cats with lower respiratory tract disease (LRTD)

Longitudinal	Control (n=34)	LRTD (n=22)	<i>P</i>
Heart rate (bpm)	182.60 ± 28.04	188.67 ± 29.45	0.519
LS <sub>1</sub> (%)	-18.69 ± 4.92	-17.16 ± 6.31	0.396
LS <sub>2</sub> (%)	-18.85 ± 4.46	-17.28 ± 4.41	0.286
LS <sub>3</sub> (%)	-15.36 ± 6.30	-13.80 ± 3.84	0.392
LS <sub>4</sub> (%)	-13.67 ± 5.37	-10.07 ± 4.05	0.031
LS <sub>5</sub> (%)	-19.84 ± 8.00	-14.05 ± 5.13	0.017
LS <sub>6</sub> (%)	-22.93 ± 10.80	-16.84 ± 5.86	0.027
LS <sub>g</sub> (%)	-18.22 ± 4.78	-14.87 ± 2.86	0.008
LSR <sub>1</sub> (s <sup>-1</sup> )	-2.23 ± 0.70	-2.03 ± 0.89	0.423
LSR <sub>2</sub> (s <sup>-1</sup> )	-2.33 ± 0.59	-1.97 ± 0.73	0.098
LSR <sub>3</sub> (s <sup>-1</sup> )	-1.87 ± 0.84	-1.70 ± 0.63	0.505
LSR <sub>4</sub> (s <sup>-1</sup> )	-1.63 ± 0.66	-1.23 ± 0.52	0.053
LSR <sub>5</sub> (s <sup>-1</sup> )	-2.42 ± 1.00	-1.70 ± 0.66	0.017
LSR <sub>6</sub> (s <sup>-1</sup> )	-2.80 ± 1.24	-1.95 ± 0.64	0.049
LSR <sub>g</sub> (s <sup>-1</sup> )	-2.21 ± 0.58	-1.76 ± 0.49	0.016
LSR <sub>E1</sub> (s <sup>-1</sup> )	1.88 ± 0.81	1.15 ± 0.55	0.088
LSR <sub>E2</sub> (s <sup>-1</sup> )	1.89 ± 0.65	1.29 ± 0.25	0.151
LSR <sub>E3</sub> (s <sup>-1</sup> )	1.55 ± 0.81	1.54 ± 0.43	0.981
LSR <sub>E4</sub> (s <sup>-1</sup> )	1.29 ± 0.82	1.40 ± 0.86	0.806
LSR <sub>E5</sub> (s <sup>-1</sup> )	1.78 ± 1.12	2.08 ± 0.72	0.594
LSR <sub>E6</sub> (s <sup>-1</sup> )	1.80 ± 1.37	2.08 ± 1.19	0.703
LSR <sub>Eg</sub> (s <sup>-1</sup> )	1.52 ± 0.73	1.59 ± 0.60	0.827
LSR <sub>A1</sub> (s <sup>-1</sup> )	1.55 ± 0.98	1.16 ± 0.38	0.465
LSR <sub>A2</sub> (s <sup>-1</sup> )	1.45 ± 0.45	0.82 ± 0.68	0.236
LSR <sub>A3</sub> (s <sup>-1</sup> )	0.92 ± 0.52	1.36 ± 0.76	0.199
LSR <sub>A4</sub> (s <sup>-1</sup> )	0.93 ± 0.55	0.26 ± 0.15	0.038
LSR <sub>A5</sub> (s <sup>-1</sup> )	1.28 ± 0.94	0.44 ± 0.57	0.096
LSR <sub>A6</sub> (s <sup>-1</sup> )	1.42 ± 1.16	1.14 ± 0.85	0.642
LSR <sub>Ag</sub> (s <sup>-1</sup> )	1.21 ± 0.57	1.04 ± 0.48	0.475

L<sub>1</sub>: basal septal, L<sub>2</sub>: mid septal, L<sub>3</sub>: apical septal, L<sub>4</sub>: apical lateral, L<sub>5</sub>: mid lateral, L<sub>6</sub>: basal lateral, L<sub>g</sub>: global, LS: peak longitudinal strain, LSR: peak longitudinal strain rate, LSR<sub>A</sub>: peak longitudinal late diastolic strain rate, LSR<sub>E</sub>: peak longitudinal early diastolic strain rate.

*P* < 0.05 (two tail), statistically significant.

**Table 7.** Comparison of left ventricular ejection volume ( $EF_{ste}$ ) and fraction area change (FAC) between clinically healthy cats (control) and cats with lower respiratory tract disease (LRTD)

	Control (n=34)	LRTD (n=22)	<i>P</i>
FAC (%)	44.63 ± 8.36	36.30 ± 6.60	0.001
$EF_{ste}$ (%)	48.81 ± 9.61	41.43 ± 10.50	0.029

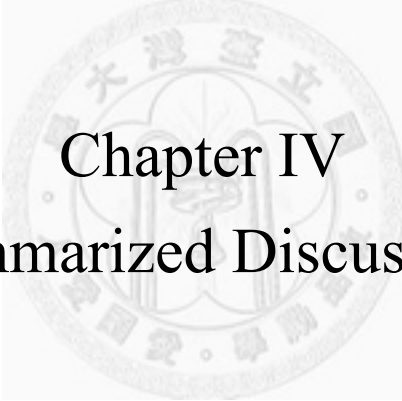
$EF_{ste}$ : Ejection fraction derived from speckle tracking echocardiography, FAC: Fractional area change derived from speckle tracking echocardiography.  
 $P < 0.05$  (two tail), statistically significant.

**Table 8.** Comparison of ventricular synchrony (RT-c $\epsilon$ , SDT-c $\epsilon$ ) and heterogeneity (SH- $\epsilon$  and TH- $\epsilon$ ) between clinically healthy cats (control) and cats with lower respiratory tract disease (LRTD)

Parameter	Control (n=34)	LRTD (n=22)	<i>P</i>
RT-c $\epsilon$ (ms)	32.49 ± 9.32	37.78 ± 20.56	0.576
RT-r $\epsilon$ (ms)	40.21 ± 28.72	46.79 ± 52.27	0.836
RT-l $\epsilon$ (ms)	44.24 ± 22.62	49.45 ± 28.34	0.530
SDT-c $\epsilon$ (ms)	11.74 ± 4.16	14.27 ± 7.55	0.481
SDT-r $\epsilon$ (ms)	16.48 ± 13.41	17.76 ± 19.45	0.752
SDT-l $\epsilon$ (ms)	19.38 ± 8.52	19.65 ± 10.90	0.933
SH-c $\epsilon$ (%)	13.05 ± 5.86	11.18 ± 7.39	0.362
SH-r $\epsilon$ (%)	19.06 ± 10.34	18.83 ± 10.30	0.942
SH-l $\epsilon$ (%)	15.38 ± 6.81	11.54 ± 6.12	0.081
TH-c $\epsilon$ (%)	-14.28 ± 4.60	-11.43 ± 3.53	0.034

RT-c $\epsilon$ : range of time to peak circumferential strain, RT-l $\epsilon$ : range of time to peak longitudinal strain, RT-r $\epsilon$ : range of time to peak radial strain, SDT-c $\epsilon$ : standard deviation of time to peak circumferential strain, SDT-l $\epsilon$ : standard deviation of time to peak longitudinal strain, SDT-r $\epsilon$ : standard deviation of time to peak radial strain, SH-c $\epsilon$ : segmental heterogeneity in circumferential strain, SH-l $\epsilon$ : segmental heterogeneity in longitudinal strain, SH-r $\epsilon$ : segmental heterogeneity in radial strain, TH-c $\epsilon$ : transmural heterogeneity in circumferential strain.

$P < 0.05$  (two tail), statistically significant.



**Chapter IV**  
**Summarized Discussion**

## **Summarized discussion**

Myocardial strain and strain rate in cats was almost independent to age, body weight and heart. However, circumferential strain was lower in male. Based on the finding of ventricular heterogeneity and synchrony circumferential strain was decreasing from subendocardium to subepicardium, and lower strain was at cardiac apex.

Systolic strain was correlated to diastolic indices in conventional echocardiography. It is indicated that systolic deformation was in associated with overall diastolic function. More cases in both diseased and clinically healthy cats are needed define the link [1].

Impact of lower respiratory tract disease on left ventricular deformation in cats was assessed. Impaired systolic and diastolic function was not detected by conventional echocardiography but myocardial strain. No change of right ventricular functions or pulmonary hypertension was detected using conventional echocardiography. It is implied that the advantage of speckle tracking echocardiography in detection of early left ventricular deformation before cardiac geometry changed by volume or pressure overloading from right heart. However, the affected segments of myocardium were in the free wall, which different from human patients with pulmonary hypertension [2-4]. The exact mechanism was not answered.

## Reference:

1. Yip G, Wang M, Zhang Y, Fung J, Ho P, Sanderson J: **Left ventricular long axis function in diastolic heart failure is reduced in both diastole and systole: time for a redefinition?** *Heart* 2002, **87**:121-125.
2. Olson N, Brown JP, Kahn AM, Auger WR, Madani MM, Waltman TJ, Blanchard DG: **Left ventricular strain and strain rate by 2D speckle tracking in chronic thromboembolic pulmonary hypertension before and after pulmonary thromboendarterectomy.** *Cardiovasc Ultrasound* 2010, **8**:43.
3. Rajdev S, Nanda NC, Patel V, Singh A, Mehmood F, Vengala S, Fang L, Dasan V, Benza RL, Bourge RC: **Tissue Doppler assessment of longitudinal right and left ventricular strain and strain rate in pulmonary artery hypertension.** *Echocardiography* 2006, **23**:872-879.
4. Ramani GV, Bazaz R, Edelman K, López-Candales A: **Pulmonary Hypertension Affects Left Ventricular Basal Twist: A Novel Use for Speckle-Tracking Imaging.** *Echocardiography* 2009, **26**:44-51.

